



UNIVERSIDAD DE CHILE
FACULTAD DE CIENCIAS FÍSICAS Y MATEMÁTICAS
DEPARTAMENTO DE GEOLOGÍA

LITHOLOGICAL CONTROLS INFLUENCING THE GEOCHEMISTRY OF GEOTHERMAL
SYSTEMS NORTH OF THE VILLARRICA VOLCANO, AN EXPERIMENTAL APPROACH

MEMORIA PARA OPTAR AL TÍTULO DE GEÓLOGO

IGNACIO JOSÉ VILLALÓN OLIGER

PROFESOR GUÍA:
DIEGO MORATA CÉSPEDES

MIEMBROS DE LA COMISIÓN:
MARTIN REICH MORALES
DOLORINDA DANIELE

Este trabajo ha sido parcialmente financiado por el Centro de Excelencia en Geotermia de los Andes (CEGA) (Fondap-Conicyt project 15090013) y el Karlsruhe Institute of Technology (KIT) (CONICYT-BMBF International Scientific Collaborative Research Program project PCCI130025/FKZ 01DN14033)

SANTIAGO DE CHILE
2015

**RESUMEN DE LA MEMORIA PARA OPTAR
AL TÍTULO DE:** Geólogo
Por: Ignacio José Villalón Oliger
Fecha: 21/08/2015
Profesor Guía: Diego Morata Céspedes

Controles litológicos sobre la geoquímica de los sistemas geotermales al norte del volcán Villarrica

En la zona norte del volcán Villarrica las unidades más relevantes en términos de dimensiones y de poder albergar sistemas hidrotermales son: 1) El Batolito Norpatagónico compuesto principalmente por granitoides del Cretácico y Mioceno 2) Las unidades volcánicas y volcanoclásticas del Cenozoico tales como las que se encuentran en la cuenca de Curamallín (Oligoceno-Mioceno), las cuales prácticamente desaparecen al sur del volcán.

Por otro lado hay distintos procesos que pueden afectar la composición de las aguas termales: mezcla, ebullición, interacción con vapores o fluidos de origen magmático, distintas fuentes del fluido que compone el reservorio, cambios de temperatura, entre otros, pero uno de los procesos más importantes que determina dicha composición es la interacción química con las unidades de roca que albergan al reservorio hidrotermal.

En este trabajo se plantea que la composición de los fluidos hidrotermales está importantemente controlada por procesos de interacción calor-fluido-roca con las unidades volcánicas y volcanoclásticas anteriormente mencionadas, por esto, con el objetivo de determinar la relevancia de los procesos de interacción con dichas rocas, se han realizado experimentos de alteración en sistemas cerrados a temperatura constante en un reactor químico. Junto con esto, se realizaron modelos geoquímicos con el fin de predecir los resultados de la alteración geotermal en las muestras seleccionadas.

Los resultados de los experimentos con reactor químico muestran similitudes con las aguas termales del área de estudio. Además, los modelos geoquímicos son consistentes con los resultados del reactor. De esta forma, la metodología experimental utilizada en este trabajo permite un mayor entendimiento de los procesos de alteración geotermal que actúan en la zona estudiada confirmando de alguna forma la relevancia de los procesos de interacción calor-fluido-roca y en particular de la interacción con las unidades volcánicas y volcanoclásticas al norte del volcán Villarrica.

Abstract

North of Villarrica volcano, the most relevant geological units in terms of dimensions and the possibility of containing a hydrothermal system are: 1) The North Patagonian Batholith, composed mainly by Cretaceous to Miocene granitoids. 2) The Cenozoic volcanic and volcanoclastic units such as the ones found in the Oligocene-Miocene Curamallín Basin. The later are almost nonexistent south of the volcano.

On the other hand, there are different processes that may affect the composition of a hydrothermal fluid: mixing, boiling, interaction with magmatic fluids or vapors, different sources for the reservoir fluid, temperature changes, among others. But one of the most important processes that determine the fluid composition is the chemical interaction with the rock units that contain the reservoir.

In this work, it is proposed that north of Villarrica volcano, the composition of the hydrothermal fluids is mainly controlled by heat-water-rock interaction processes with the volcanic and volcanoclastic rock units. For this reason and with the aim of determine the relevance of heat-water-rock interaction processes with the mentioned units, closed system alteration experiments were performed at fixed temperature using rock samples from the area. Also, with the aim of predicting the results of hydrothermal alteration on the selected samples, geochemical models were performed.

Experimental results show a good similarity with the thermal waters from the Villarrica area. Additionally, geochemical models are consistent with the hydrothermal reactor experiments. Consequently, the experimental approach used in this work allows a better understanding of the geothermal alteration processes active in the studied area and, to a certain degree, confirms the relevance of heat-water-rock interaction processes with volcanic and volcanoclastic units north of the Villarrica volcano.

Acknowledgements

I wish to express my sincere thanks to “Centro de Excelencia en Geotermia de los Andes (CEGA)” (Fondap-Conicyt project 15090013) and Karlsruhe Institute of Technology (KIT) (CONICYT-BMBF International Scientific Collaborative Research Program project PCCII30025/FKZ 01DN14033) for their financial support in this thesis. Likewise, I take the opportunity to express my gratitude to my supervisors Dr. Diego Morata, Dr. Martin Reich and Dr. Linda Daniele. A very special thanks to Sebastian Held and Fabian Nitschke whose constant help, motivation and cheering, made this thesis possible. I am also grateful to all the people that advised me and encouraged me in multiple occasions such as Diego Aravena, Mauricio Muñoz, Pablo Sánchez, Verónica Rodríguez and Mercedes Vázquez. And last but not least, I thank all those who directly or indirectly have lent me their help in the process, especially to Tatiana Reyes and my parents, Pauline Oligier and Augusto Villalón.

Index of contents

1	Introduction	1
1.1	Hydrothermal systems	1
1.2	Local context.....	1
1.3	Water rock interaction processes	2
1.4	Alteration experiments and geochemical models	3
2	Objectives	4
3	Previous works	6
3.1	Geothermal studies from the area	6
3.2	Heat water rock interaction.....	6
3.3	Alteration experiments.....	7
4	This work.....	9
5	Geological setting.....	10
5.1	Geodynamic setting	10
5.2	Mesozoic and Cenozoic stratigraphy.....	11
5.3	Thermal waters	12
6	Methodology.....	16
6.1	Rock sampling	16
6.2	Petrography: Starting materials for geochemical models	16
6.3	Batch reactor tests	17
6.4	Modeling	20
6.5	Nomenclature.....	24
7	Results	25
7.1	Mineralogy.....	25
7.2	SEM-EDS	25
7.3	XRF.....	27
7.4	Mass balance.....	27
7.5	Alteration experiments: exp(IV-4).....	28
7.6	Modeling	29
8	Discussions	31
8.1	Petrography.....	31
8.2	Alteration experiment results.....	32
8.3	Analysis of boundary conditions sensitivity for geochemical models.....	36

8.4	A general overview of the results: comparison between batch reactor experiments, modeling results and thermal waters in the area.....	38
9	Conclusions	39
10	Bibliography	40
11	Appendix	45
11.1	Outcrop and hand sample descriptions.....	45
11.2	Thin sections descriptions	54
11.3	Results of XRD analysis	63
11.4	Matlab code used to obtain logK for glass	66
11.5	Phreeqc Models input.....	67
11.6	Detailed water composition of alteration experiments: blind and exp(IV-4).....	70

1 Introduction

1.1 Hydrothermal systems

From a general point of view, hydrothermal systems can be defined by two main components: a heat source and a hydrothermal fluid which includes solutions from different possible sources such as magmatic, metamorphic, meteoric or connate waters and also seawater. As well, this fluid resides in a permeable reservoir composed by fractured rocks or a permeable lithology. In this setting, not only mineral deposits occur due to changes in the physicochemical conditions which dynamically shift permeability and flow paths, but also alteration of reservoir rocks take place as a consequence of chemical disequilibrium with the thermal fluids. This translates into the formation of new, (meta)stable, mineral phases and changes in the fluid chemical composition (Pirajno, 2009).

On top of this, other processes can take place that change the composition of the hydrothermal fluid such as mixing, boiling, interaction with magmatic fluids or vapors, different sources for the reservoir fluid, temperature changes etc. which will result in the measured compositions of the water samples taken from springs or wells.

1.2 Local context

The Andean geological context is favorable for the presence of magmatic influenced geothermal systems in terms of heat and mass source, being volcanism and hot springs along the Andean volcanic belt the most conspicuous superficial manifestations of this relationship. In addition to the fact that magmatic fluids can be a direct source of heat and fluids for the hydrothermal system, absorption of magmatic vapors into deeply circulating groundwater (e.g. meteoric waters) produces acid waters which turn to be more aggressive in terms of rock dissolution and therefore promoting rock alteration processes.

Chile, contextualized in the present-day global energy crisis and currently dependent of fossil fuels, needs to diversify its energy matrix. Geothermal energy seems to be a realistic option that has been proven to be economically viable in other developing countries such as El Salvador, Costa Rica, Guatemala, and Nicaragua (Asturias, 2012; Mayorga, 2005; Protti, 2010; J. A. Rodríguez & Herrera, 2005). That said, the importance of available studies for specific geothermal systems is to promote and facilitate future exploration and exploitation projects, not only in electric generation but also direct use of geothermal heat.

1.3 Water rock interaction processes

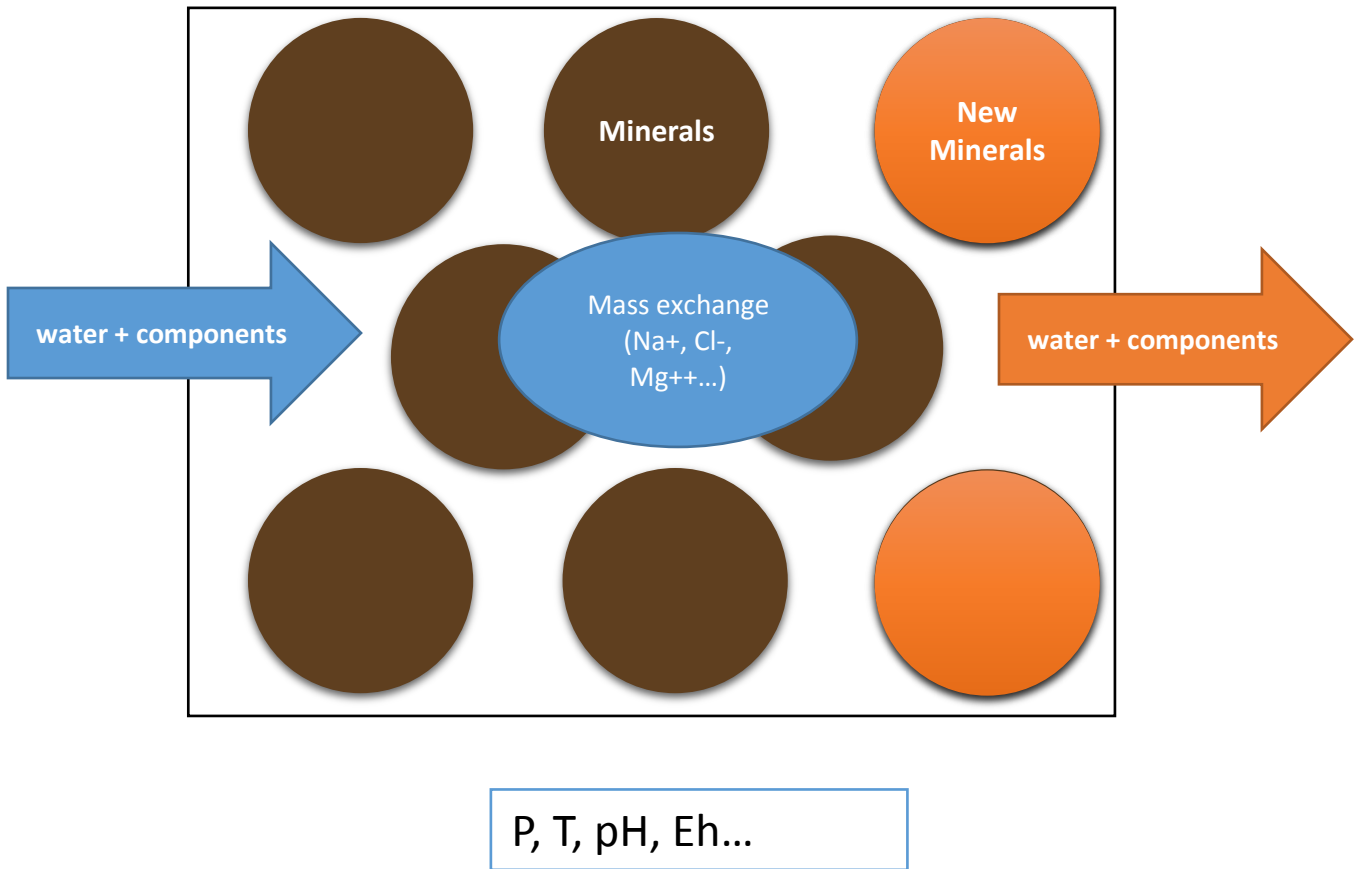


Figure 1: schematic diagram of heat-water-rock interaction processes that occur in natural hydrothermal systems. The figure shows an initial fluid (left arrow) composed by water and components such as SiO₂, Fe, Al... which interacts exchanging mass with a rock (circles) in a system with specific physicochemical conditions resulting in a new fluid (right arrows) with a different composition and also new mineral phases in the rock (completely new phases or a different amount of the same phases). If this process reaches a steady state, it is said that the system is in equilibrium (or a metastable equilibrium, that is, even if it does not change, it is not reaching a full thermodynamic equilibrium in terms of chemical potential)

Heat-water-rock interaction is a process that takes place in many natural environments including hydrothermal systems. It comprises the dissolution and precipitation reactions that occur between solid phases and a fluid composed by water and components such as SiO₂, Cl⁻, CO₃²⁻, Fe²⁺, Fe³⁺, Al³⁺, K⁺, Mg²⁺ and Na⁺ among others, which exist as species in solution (Figure 1). The later can be stoichiometrically the same as the components (e. g. SiO₂(aq), K⁺, Mg²⁺) or a combination of two or more of them (e. g. KCl, NaCO₃⁻, MgCl⁺), but the composition of a solution is sufficiently expressed as its components. On the other hand, speciation of those components will be a result of the physicochemical conditions for a particular system (Bethke, 2008).

For a closed system, when pressure and temperature are fixed, a thermodynamic equilibrium is reached when all the chemical reactions in a system reach a steady state in which any disturbance away from the equilibrium will be counteracted restoring the conditions in the steady state. In spite of the fact that closed systems are not to be found in natural environments; depending on the space and time scale, this approach can be a good approximation of what could be expected in such conditions.

1.4 Alteration experiments and geochemical models

In this setting, water-rock interaction experiments using a hydrothermal batch reactor in combination with geochemical models are implemented as an indirect approach of heat-water-rocks interaction processes that could happen in active geothermal systems. Moreover, the comparison of results from geochemical models with the alteration experiments and the thermal water samples from the area allows constraining the chemical evolution of the thermal water in the system, assessing not only the relevance of water rock interaction processes in the resulting water composition but also the relevance of different rock units in the process.

To do so, several rock samples were collected and petrographic analysis were performed, subsequently the sampling site most likely to have geothermal reservoir rock was selected for closed system alteration experiments at fixed temperature, reacting the rock samples with water. Also, with the purpose of predicting the results of hydrothermal alteration on the selected samples, geochemical models were performed

2 Objectives

There are different processes that may affect the composition of a hydrothermal fluid: mixing, boiling, interaction with magmatic fluids or vapors, different sources for the reservoir fluid, temperature changes, among others. But one of the most important processes that determine the fluid composition is the chemical interaction with the rock units that contain the hydrothermal reservoir.

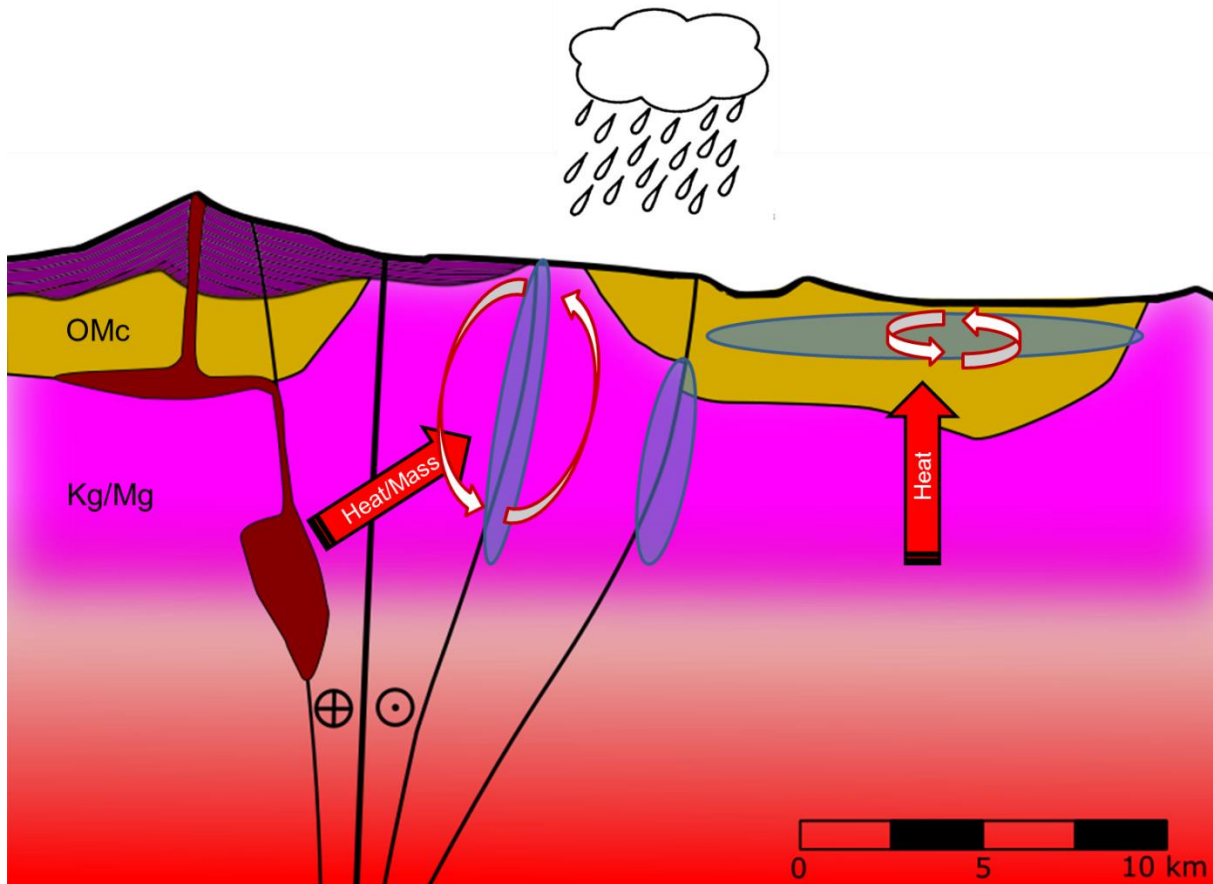


Figure 2: schematic SW- NE section of the main features found at the area of interest. As a simplified geology, the north Patagonian Batholith (Mg/Kg) acts as a basement for Oligocene and Miocene volcanic and volcanosedimentary units (OMc). Possible processes occurring in the area are depicted in the scheme: deep circulation of water in fault zones or in permeable volcanic and volcanoclastic units, magmatic intrusions as a mass and heat source, greater geothermal gradient and meteoric water as input.

From a general perspective, there are two possible reservoir rocks north of Villarrica volcano: the North Patagonian Batholith (Kg/Mg), composed mainly by Cretaceous to Miocene granitoids and secondly, the Cenozoic volcanic and volcanoclastic units (OMc) such as the ones found in the Oligocene-Miocene Curamallín Basin (Figure 2). The later, almost nonexistent south of the volcano is the starting material

for this work and so, it is proposed that, north of Villarrica volcano, the volcanic and volcanoclastic units play a relevant role in the composition of the hydrothermal fluids; and furthermore, that this composition is mainly controlled by heat-water-rock interaction processes.

Consequently the main objective of this thesis is assessing the relevance of water-rock-interaction processes between thermal waters and volcanic and volcanoclastic units north of Villarrica volcano.

Secondary objectives are: mineralogical and chemical characterization of representative rock samples from volcanic and volcanoclastic units in the studied area; determine the alteration phases that might be occurring in natural hydrothermal systems from the area; analyze and compare the models, experiments and natural waters to evaluate the feasibility of the proposed methodology and geochemical models (Figure 3).

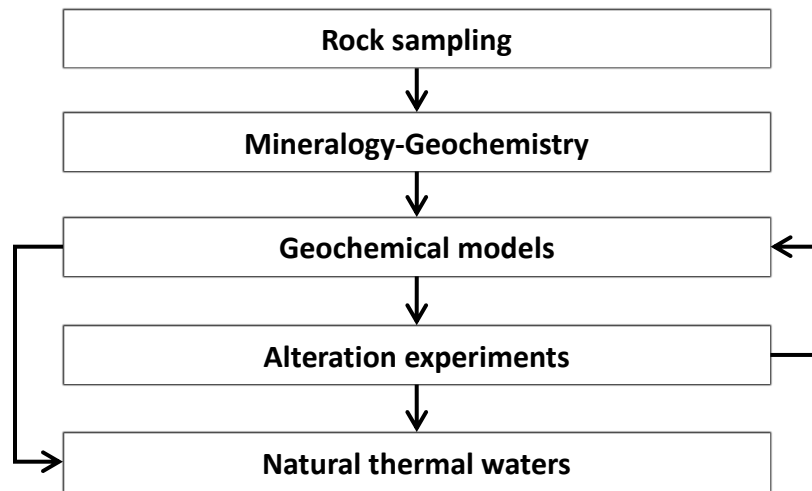


Figure 3: scheme of activities necessary to achieve the proposed objectives

3 Previous works

3.1 Geothermal studies from the area

The Southern Volcanic Zone in Chilean Andes has a lot of remarkable features concerning geothermal exploration. Several studies are today available about the geothermal systems found in this area, but most of these studies are focused on describing thermal water chemistry (Hauser Y., 1997; Pérez, 1999; Risacher, Fritz, & Hauser, 2011; Risacher & Hauser Y., 2008). As well, some recent studies have encompassed the relationships between structural control and water geochemistry (Held et al., 2015; Sánchez, Pérez-Flores, Arancibia, Cembrano, & Reich, 2013; Tardani et al., 2015). Nevertheless, many questions are always present for a complete understanding of the different processes related to these geothermal systems.

3.2 Heat water rock interaction

Heat-water-rock interaction in hydrothermal environments can be studied using two different approaches: empirically and thermodynamically. The first approach is related to studies of alteration mineralogy and associated processes for specific geothermal systems around the world (e.g. Browne, 1978; Hellevang, Dypvik, Kalleson, Pittarello, & Koeberl, 2013; Kristmannsdottir, 1979; Lagat, 2010; Reyes, 1990). Since they are a compilation of well data from different geological contexts and thermodynamic conditions, they serve as a guide for rock alteration experiments and exploration of unperforated geothermal systems.

Another method is to use thermodynamics to predict and understand possible alteration processes in a system (Anderson, 2009; Bethke, 2008). To determine the equilibrium state of a system, it is necessary to have a thermodynamic database with the equilibrium constants of all the reactions taking place in the system at the specified temperature. More of this can be found at geochemical modeling section in the methodology.

Today it is possible to find such thermodynamic databases like the `lnl.dat` database by the Lawrence Livermore National Laboratory, or `phreeqc.dat` (Parkhurst & Appelo, 2013) and also specialized software which will solve the equation system that results from considering all the reactions that take place in a system with various components. Examples of this are PHREEQC (Parkhurst & Appelo, 2013), GWB (Bethke & Yeakel, 2015), GEMS (Kulik et al., 2013; Wagner, Kulik, Hingerl, & Dmytrievava, 2012), EQ3/6 (Wolery, 1992), ChemApp (Eriksson, Hack, & Petersen, 1997; Petersen & Hack, 2007), HCh (Bastrakov & Shvarov, 2007) among others. They differ in price, user interface, specific tools and other features, but, if using the same database, all these computer programs should give similar results for simple thermodynamic equilibrium calculations.

3.3 Alteration experiments

A more empirical approach is recreating the conditions of part of a natural system at laboratory scale in order to measure the result of rock dissolution and alteration in a controlled environment.

Pérez-Zárate, Torres-Alvarado, Santoyo, & Díaz-González (2010) not only show that Na/K geothermometer revision by Díaz-González et al. (2008) fails to predict the temperature in batch experiments for temperatures lower than 200°C, especially when no NaCl is added (differences are as high as 408%) but also, they analyze a great amount of works which had used this methodology, assessing the relevance of the principal variables affecting water-rock interaction experiments. So the next paragraphs will be a summary of the results and references presented in this work. If the reader wants to delve into this topic, reading this work is highly recommended.

The first systematic fluid-rock interaction experiments were performed by Hawkins & Roy (1963) and Ellis & Mahon (1967). The later reacted basalt, andesite and dacite with pure water at temperatures between 150 and 350°C for a maximum of 12 days. They observed that Na and K concentrations in solution were a function of temperature and rock type and also found that alkali concentration increased with reaction time but K was liberated faster than Na. As well, Ellis (1968) shows that when reacting andesites at 400°C, high NaCl-rich solutions greatly enhance the dissolution of some metal ions like B, Mg, Al, Mn, Fe, Cu, and Pb. Other works worth mentioning that that have used this methodology are Dickson & Potter (1982); Gislason & Eugster (1987); Gislason, Veblen, & Livi (1993); Hajash & Archer (1980); Heimann, Beard, & Johnson (2008); Kacandes & Grandstaff (1989); Liu, Suto, Bignall, Yamasaki, & Hashida (2003); Robert & Goffé (1993); D. Savage & Chapman (1982); David Savage, Bateman, & Richards (1992); Seyfried & Bischoff (1979); Shiraki & Iiyama (1990); Stoffregen & Cygan (1990).

As well, alteration experiments have been used to study solute geothermometers, quantifying dissolution rates of some minerals and studying the chemical evolution of the reacted fluid in controlled conditions. Examples of this are: Potter, Dibble, Parks, & Nur, (1982) who studied the Na/K geothermometer reacting oligoclase and microcline with fluid containing 100 ppm NaCl. They found that these experiments needed a long time to get to a steady state. Subsequently, Benjamin, Charles, & Vidale (1983) using the data compiled by Fournier & Truesdell (1973) and merging it with their own experiments, proposed now constants for the Na-K-Ca geothermometer concluding that feldspar and quartz are not the mineral assemblage that control solution composition, instead, they found that reactions involving clays and zeolites were controlling this. Additionally, David Savage (1986) reacted granite with water at 100°C and 500 bars for 203 days. Na and K reached steady state after 10 days but Na/K geothermometer indicated a temperature between 500 and 600°C and NA-K-Ca geothermometer (R.O. Fournier & Truesdell, 1973) yield a temperature of 190°C.

It is important to mention that many of the works analyzed by Pérez-Zárate et al. (2010) are concerned about geothermometers, rock alteration processes in general, the effect of different variables such as pH or NaCl content of the fluid, among others, but it is seldom used to approach a specific natural system in order to assess the relevance of different rock units.

According to Pérez-Zárate et al. (2010) when analyzing the works of Hajash & Archer (1980) and Brantley & Chen (1995) it is possible to define the main variables affecting water-rock interaction experiments. These variables are: temperature, experimental system, water/rock ratio, rock grain size, fluid and rock initial compositions, sampling techniques and reaction time. Their analysis shows that perhaps temperature and reaction time are the most important variables for water-rock interaction, at least when trying to simulate the conditions of natural systems, followed by rock type and of course fluid and rock initial compositions. Also the water/rock ratio is relevant to efficiently achieve equilibrium, therefore a water/rock ratio of $W/R=3$ would be recommendable, allowing the system to reach equilibrium during the first 1000 hours of reaction, while a ratio of $W/R=10$ takes too long for the timescale considered for the experiments. Grain size is also relevant to achieve equilibrium since it directly affects the dissolution rate by increasing the reactive surface although diffusion of some elements can be a relevant factor. Finally, even though reaction time is dependent of the experimental conditions, at least 1000 hours (~40 day) are recommended.

On the other hand, Rodríguez (2011) using reaction path simulations and also batch experiments determines the resulting geochemistry and mineralogy of the interaction between silicic volcanic rocks and a fluid of 240°C. His results give insights to the effects of extent of reaction on silicic rock alteration and the associated water chemistry under geothermal conditions; they show that extended rock leaching is necessary for the formation of secondary minerals commonly associated with geothermal alteration (~100 days). Nevertheless Hellevang et al. (2013) performs alteration experiments on impact melts from El'gygytgyn and volcanic glasses (rhyolites and basalts) from Iceland and show that less silicic volcanic rocks react much faster.

4 This work

In this work the aim is to find the link between reservoir rock and fluid composition, particularly for volcano-sedimentary rocks (medium silica contents) from the studied area.

As stated in Pérez-Zárate et al. (2010), a relatively low water/rock ratio is needed to be able to reach a steady state in most reactions involving water rock interaction, therefore, as recommended, a 3:1 water:rock ratio was used. As well, in the same work, Pérez-Zárate et al. conclude that at least 1000 hours (~41 days) of reaction time are recommended, but as stated before, Rodríguez (2011) concludes that for more silicic rocks at least 4000 (~166 days) hours are needed. For those reasons the long term experiments were conducted to a maximum of 180 days.

The temperature chosen for the experiments and modeling was 140°C. Even though (Held et al., 2015) shows that most of the geothermometry temperatures using $d^{18}O$ isotopes at SO_4 and H_2O north of Villarrica volcano are between 110 and 130 °C, by personal communications with him it was possible to obtain the unpublished data for springs that are in the direct vicinity of the studied area and this shows that temperatures for Pangui and Toledo springs are 139 and 138 °C respectively. Also (Sánchez et al., 2013) shows that cation geothermometers temperatures are between 100 and 180°C, although cation geothermometers might be affected by dilution given the high amount (>2000 mm/year) of annual precipitations in the area (Dirección General de Aguas (DGA), 1987). Figure 6 shows cation geothermometer results for thermal waters in the area.

In addition to the batch experiments, a Phreeqc (Charlton & Parkhurst, 2011; Parkhurst & Appelo, 2013) equilibrium model was used to better understand the reactions in the water-rock interactions from the area of study. As well, mineral stability graphs and activity calculations were performed using the student edition of the Geochemist's Workbench (Bethke & Yeakel, 2015). The aim of the geochemical modellings is to validate and complement the batch experiments. In order to maintain the same conditions as in the batches, all geochemical models have the same Water:rock proportions as in the batch experiments.

Determination of present mineral phases on rock samples was made using petrographic microscope analysis, X-ray diffraction and fluorescence and also SEM-EDS.

Finally, this work will only consider the interpretations of major elements in the experiments and modeling, although trace elements are also shown as a result of Batch reactions.

5 Geological setting

5.1 Geodynamic setting

The Villarrica Volcano is located at the Southern Volcanic Zone (SVZ) which is situated on the convergent margin of Nazca and South American plates between 33°S and 46°S (Figure 4). A major structural feature in this region is the intra arc Liquiñe-Ofqui Fault System (LOFS) that extends from 38°S to 47°S in a transpressional dextral tectonic regime (Cembrano & Lara, 2009).

According to Cembrano & Lara (2009), the Villarrica volcano along with Quetrupillán and Lanín volcanoes are controlled by a NW striking, inherited basement structure. However, the volcano presents NE-trending flank vents and also is located almost above the main trace of LOFS (Figure 7).

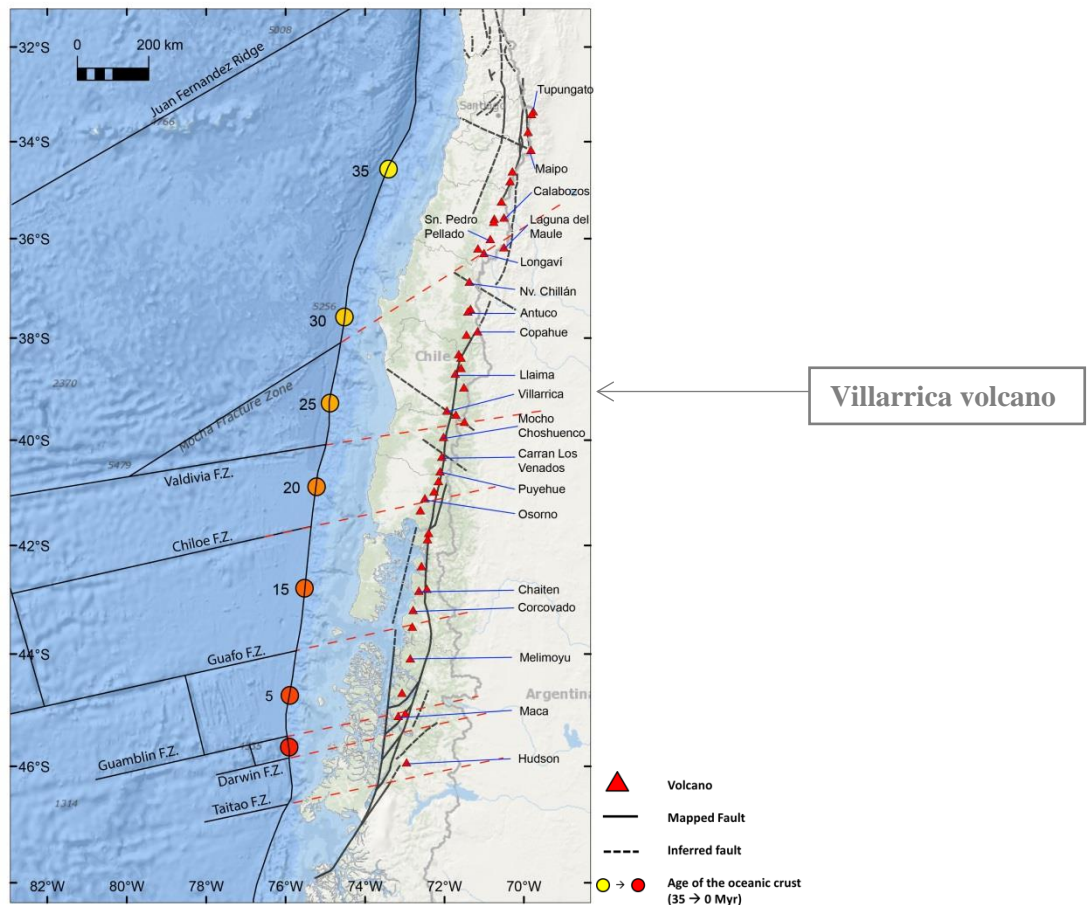


Figure 4: Tectonic setting of SVZ showing oceanic crust fault zones, crustal age at the trench, distribution of volcanoes at the SVZ, LOFS (vertical continental fault system) and NW striking inherited basement structures. From Aravena (2014)

5.2 Mesozoic and Cenozoic stratigraphy

As stated in Moreno & Lara, (2008), overlaying covered metamorphic complexes of Upper Paleozoic to the Jurassic ages together with the rift Triassic deposits, there is a sequence of Mesozoic and Cenozoic units that outcrop on the studied area. Acting as a crystalline basement for younger units, a Cretaceous magmatic arc forms plutonic longitudinal NS strips. Over this plutonic basement, intra-arc basins of Paleocene (Estratos de Relicura) and Oligocene-Miocene (Curamallín Formation) ages were developed. As well, genetically associated with the present-day tectonic setting, the Miocene magmatism is represented by several intrusive bodies with ages that range from Lower Miocene to Lower Pliocene. Also Pliocene volcanism is represented by the Curarrehue Formation. Finally, the current volcanic arc and recent glaciation deposits act as a voluminous Quaternary cover.

It is remarkable that the intense glacial erosion from the late Pliocene to late Pleistocene contributed significantly to the plutonic arc exhumation, resulting in the complex geology found in the area. South of the volcanic chain the North Patagonian Batholith (Cretaceous to Miocene intrusive units, figure 7) is present over a huge area with rocks of dioritic - granitic composition. North of the volcanic chain the outcrops of the Batholith vanish slowly. The granitoids are replaced by basin fillings of volcano-sedimentary formations covering huge areas between 34°-39° south with thicknesses up to 3km (Sernageomin, 2003).

In this study the focus is on the alteration processes of the volcano-sedimentary unit while the alteration of granitic reservoir rocks is done simultaneously in other studies, therefore, a more detailed description of the sedimentary and volcano-sedimentary units is presented below.

Relicura Formation (Par)

Composed by tuff, breccia and lavas, with very few levels of sedimentary rocks. Its outcrops are very close to Menetué, Trancura, San Luis and El Toro hot springs and also to Quimey-co, Huife and Los pozones. (OM2c in figure 7)

Curamallín Formation (OMcm)

Intra-arc basin deposits composed by tuff, volcanic breccia and andesite lavas, locally intercalated by mudstones, siltstones and sandstones. (OM2c in figure 7)

Pino Huacho Formation (Omeph)

By some authors considered to be part of the Curamallín Formation, composed by lavas and lapilli tuff breccia, arranged in layers of 3 to 5 meters. Its outcrops are located mainly on the western flank of the volcano. (Part of OM2c in figure 7)

Curarrehue Formation (Pc)

A Pliocene volcano-sedimentary unit, composed mainly by tuff, breccia and lavas, with a few levels of sandstone, limestone and shale. Its outcrops are very close to Menetué, Trancura, San Luis and El Toro hot springs. (PPI3 in figure 7)

Estratos de Huincacara (PPleh)

A sedimentary unit, composed by epiclastic conglomerates, sandstones and breccia. Its outcrops emerge only in the western flank of the Villarrica volcano. (PI3 in figure 7)

5.3 Thermal waters

Several springs over 40°C can be found in the studied area as seen in table 1. Thermal waters in this area have a tendency to steam heated waters chemistry (Figure 5) although their pH values are generally between 7 and 10. The B/Cl ratio of waters generally is higher the closer they are to the Villarrica volcano (Figures 6 and 7), which suggest a more magmatic influence in the chemistry of the waters (Sánchez et al., 2013). However, Held et al. (2015) doubt a major volcanic impact on the fluid evolution highlighting the role of fault zones for the geothermal processes in that area. In addition, cation geothermometers result in temperatures between 100°C and 180°C for the most waters in partial equilibrium (Figure 6).

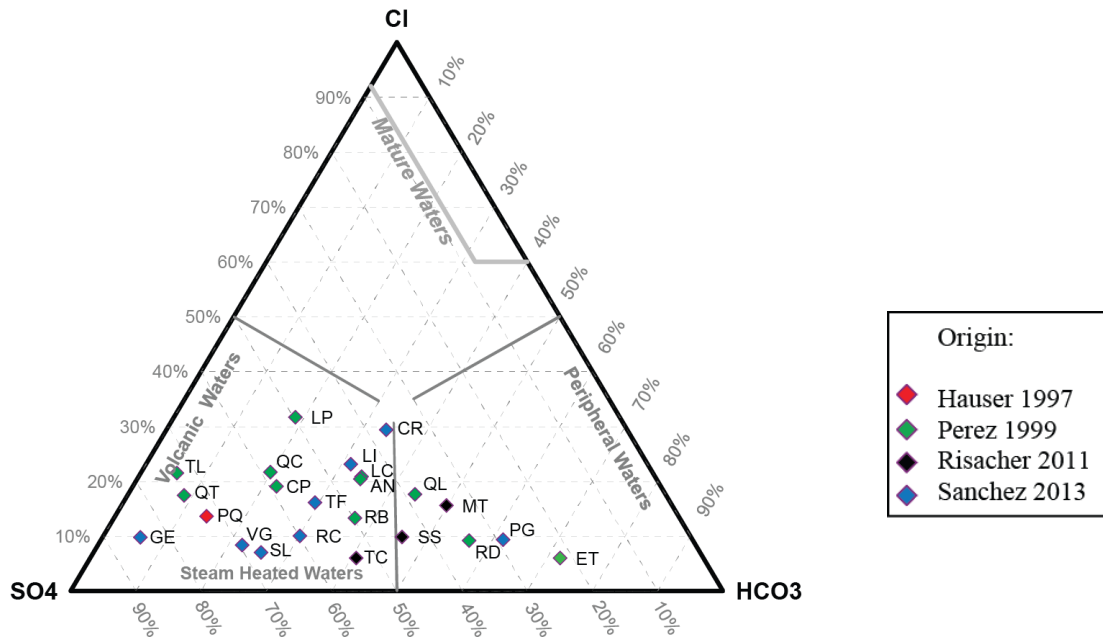


Figure 5: Geochemical classification of the thermal waters in the vicinity of Villarrica volcano. Made with Powell & Cumming (2010) spreadsheet.

Table 1: temperature and pH of hot springs in the vicinity of Villarrica volcano

Sample Name	Origin	Sample Label	Temp C	pH
Ancamil	Perez 1999	AN	40	7.4
Ex-Trancura (Copiupulli)	Perez 1999	CP	29	8.0
Conaripe	Sanchez 2013	CR	68	8.6
El Toro (Maichén)	Perez 1999	ET	17	7.4
Geometricas	Sanchez 2013	GE	72.4	8.4
Liucura	Perez 1999	LC	29.5	7.9
Liquine	Sanchez 2013	LI	29	7.38
Los Pozones	Perez 1999	LP	52	8.91
Menetue	Rischer 2011	MT	43.9	8.23
Palguin	Sanchez 2013	PG	35.5	8.7
Pangui	Hauser 1997	PQ	48	6.9
Quimey-Co	Perez 1999	QC	51	9.2
Pozos de Culán	Perez 1999	QL	41	7.4
Quintomán	Perez 1999	QT	65	9.3
Rio Blanco	Perez 1999	RB	70	8.3
Rincon	Sanchez 2013	RC	35.7	8.0
Rinconada	Perez 1999	RD	40	6.88
San Luis	Sanchez 2013	SL	39.3	9.4
San Sebastian	Rischer 2011	SS	44.9	7.47
Trancura	Rischer 2011	TC	34.2	7.7
Trifupan	Sanchez 2013	TF	37.3	8.9
Toledo	Perez 1999	TL	42	7.46
Vergara	Sanchez 2013	VG	40.7	7.8

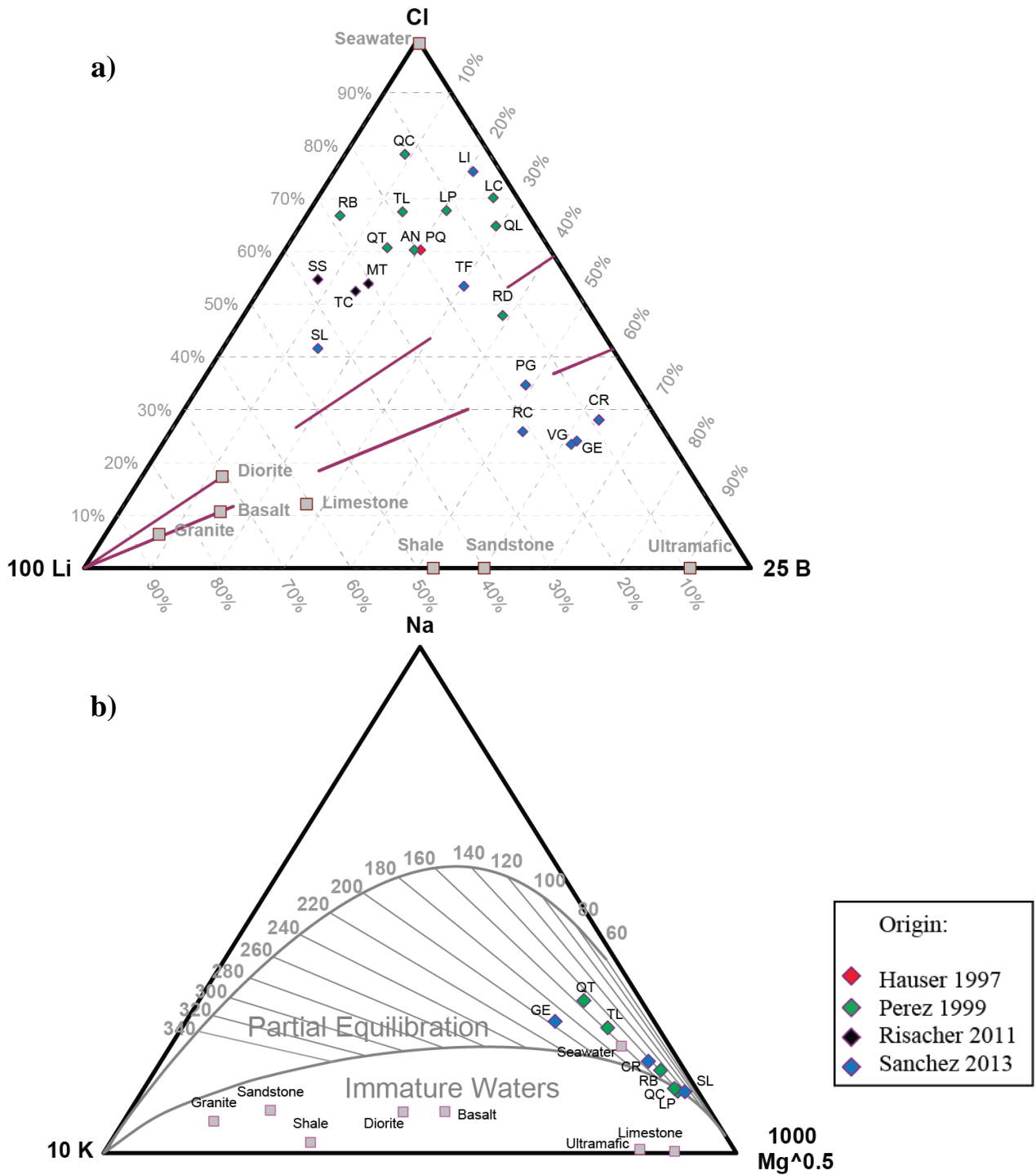


Figure 6: Li-Cl-B (a) and K-Na-Mg geothermometer (b) diagrams for geothermal waters in the vicinity of Villarrica volcano (Powell & Cumming, 2010). Thermal water data from Hauser Y., 1997; Pérez, 1999; Risacher et al., 2011; Sánchez et al., 2013.

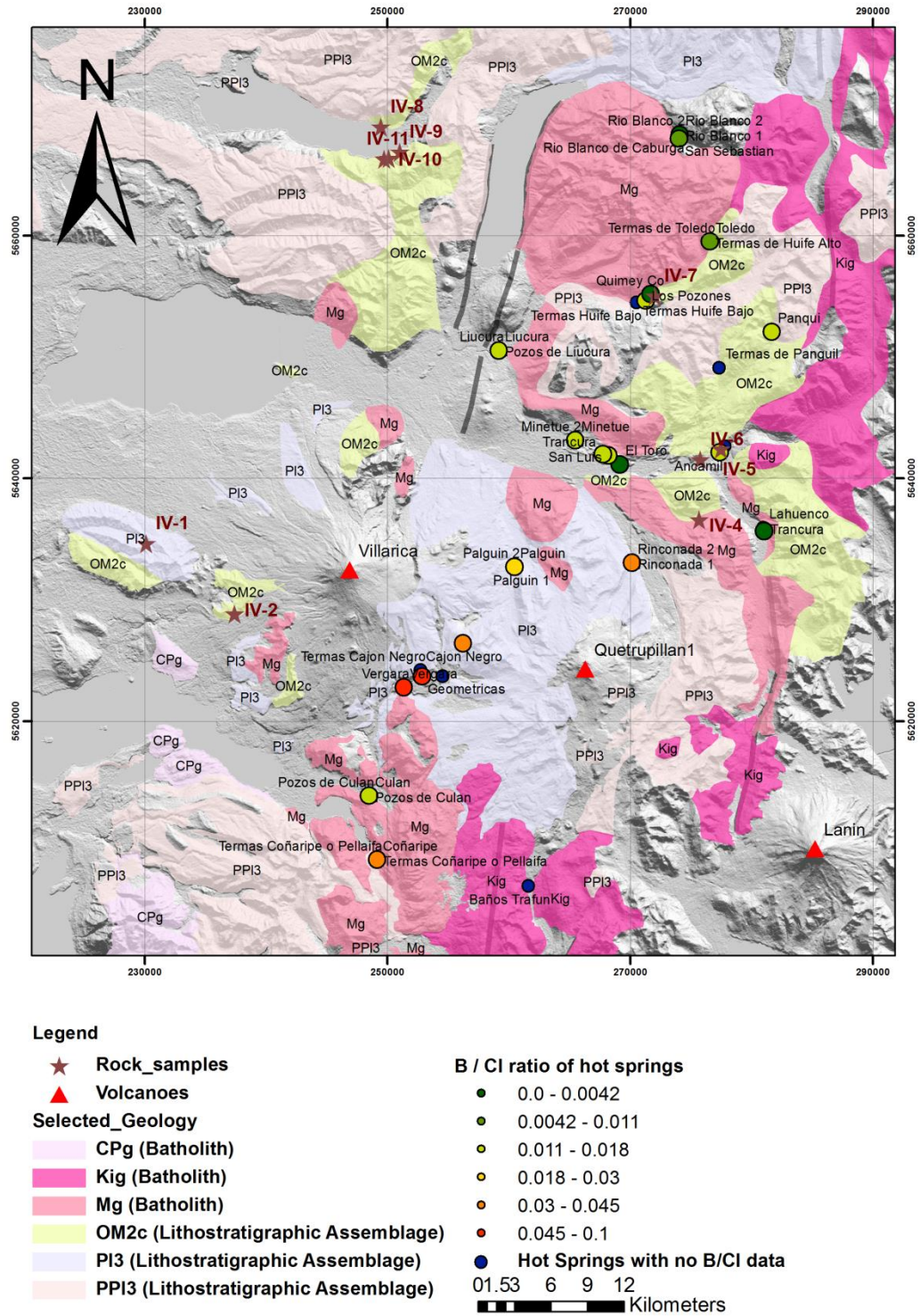


Figure 7: Rock sample distribution and B/Cl ratio of thermal springs surrounding the Villarrica area, higher ratios can be related to a magmatic input (Sánchez et al., 2013). Geology modified from (Sernageomin, 2003), thermal water data from Hauser Y., 1997; Pérez, 1999; Risacher et al., 2011; Sánchez et al., 2013 as listed in table 1.

6 Methodology

6.1 Rock sampling

Nine volcanic-sedimentary rock samples were collected and a petrographic analysis was performed. At least 2 kg of apparently non-weathered rock were sampled from each location. Three zones were considered for sampling: southwest of Villarrica volcano (IV-1 & IV-2), where Pino Huacho and Estratos de Huincacara Formations are the dominant sedimentary units; north of the volcano (IV-8; IV-9; IV-10 & IV-11), where Curamallín Formation is present and northeast of the volcano (IV-4; IV-5; IV-6 & IV-7), where Curarrehue and Relicura Formations are present (Figure 7). This last zone was the most interesting for potential reservoir rocks since it has most of the favorable factors to hold a geothermal reservoir, such as permeable rocks, proximity to heat source, intense faulting and most importantly, high temperature thermal springs in the direct vicinity.

6.2 Petrography: Starting materials for geochemical models

To each sample, thin section, XRF and an XRD analysis were performed in order to determine the present mineral phases to be used in the modeling and to decide on which sample the experimental alteration studies will be conducted.

6.2.1 Thin sections

All samples were analyzed with a petrographic microscope and the following information was obtained when possible: primary and alteration mineralogy (abundance, size, shape and observations), and also a general description of the rock including at least one photomicrography.

6.2.2 XRD

An XRD (Siemens D5000 X-ray diffractometer, Universidad de Chile) analysis was performed in order to better characterize the rock samples in terms of their mineral phase composition. From each rock at least 60 g of powder was obtained from an agate mortar grinder, nevertheless this portion was homogenized with at least 300g of sample that were previously reduced to < 2 mm fragments with a jaw crusher.

Ultimately, it was possible to confirm or improve the mineralogy obtained from the thin section analysis but the high amount of false positive possible identifications (derived from peak superposition in the identification process) implied that only expected mineralogy was taken into account.

6.2.3 XRF

For the investigation of the bulk rock chemical composition an X-ray fluorescence analysis was conducted using a S4-Explorer from Bruker AXS (KIT, Germany). Geochemical data obtained were used to perform a mass balance in order to better constrain the mineralogy of selected rocks.

6.2.4 Mass balance

In order to use the most adequate mineralogy for the Phreeqc model, a mass balance was performed to the final mineral proportions using the whole rock XRF results. This means that the bulk composition of the rock should be reflected by the compositions and proportions of each mineral.

To do that, the first thing was fixing the proportions for the minerals that had elements which could only be explained by 1 mineral phase. Then, the rest of the mineral proportions were somewhat arbitrarily changed the closest possible to the original mineralogy obtained by petrography with a maximum difference in composition of $\pm 5\%$ in concentration (mass proportion) for each element.

6.3 Batch reactor tests

Batch reactor tests enable the investigation of water-rock interaction processes under in situ reservoir condition at the laboratory scale.

6.3.1 Sample preparation

As discussed in the previous works section, there are many factors involved in the reaction rate and the time needed to reach equilibrium. Since it is very difficult to consider all the factors to model a natural system and also since at a natural scale it might take a long time, the aim was to prepare the samples in order to maximize contact surface and, therefore, minimize the time needed to reach a steady state. Rock samples were grinded to powder with particles smaller than 0.063 mm.

The rocks were carefully cleaned so that no weathered rock remains in the sample. Initially the rocks are reduced to <2 mm with a jaw crusher, then pulverized for 10 minutes in an agate mortar grinder and

finally passed through a 0.063 mm sieve. If a portion of the rock does not fit through the sieve, it is pulverized again in the agate mortar until the entire sample is smaller than 0.063 mm. At the end all powder is passed through a sample homogenizer (Figure 8).



Figure 8: powder sample homogenizer machine working.

6.3.2 Assembling the batch reactor

A V4A steel, completely hermetic vessel is used (Figure 9). Once the powder is ready, the batch reactors (vessels) are carefully cleaned with ultrapure water and assembled for the tests. 40.00 g of rock powder and approximately 120 ml of double ultrapure water are inserted on each vessel. Finally the batch reactors are placed inside an oven with desired temperature and for a specific amount of time.



Figure 9: a batch reactor vessel used in the experiments

6.3.3 Water analysis

After the extraction, the fluid samples are centrifuged, then filtered and a series of analysis are made to the resulting water:

- Physicochemical parameters are measured after opening the batches (pH, REDOX, alkalinity (titration) and conductivity)
- A Thermo Fisher Scientific XSERIES II ICP-MS is used to determine cation concentrations in the water. Specifically for Li, B, Na Mg, Al, P, K, Ca, Ti, V, Cr, Mn, Fe, Co, Ni, Cu, Zn, As, Rb, Sr, Mo, Cd, Sb, Cs, Ba, Pb & U.
- A Dionex ICS 1000 Ion chromatographer is used for anions: F, Cl, Br, NO₃, PO₄, SO₄, HCO₃ & CO₃.
- A Perkin Elmer UV/VIS spectrometer for SiO₂

To avoid miscalculations by precipitation in the resulting waters, acidified and diluted samples were also analyzed. Once the water from the batches is extracted, centrifuged and bottled, two additional bottles are filled for each experiment; the first one is diluted with pure water by a factor of 3 and to the second one acidified with concentrated nitric acid. Finally, after the results were out, the highest values for each element is the one used for later interpretations.

Due to the limited time and resources available, only rocks from the sampling site IV-4 were selected for complete time series experiments, with 10, 20, 30, 45, 60, 90, 120 and 180 days experiments.

6.3.4 Batch reactor pressure

Considering the thermal expansion of liquid, thermal expansion of the vessel, compressibility of the liquid and increase in volume of the vessel, the pressure inside the vessels should be:

$$(a_f - a_v) * \frac{dT}{B + \frac{D}{tE}} \sim 5.8 \text{ Bar}$$

Where:

Volumetric CTE of the fluid (a_f) = $0.00021^\circ\text{C}^{-1}$

Volumetric CTE of the vessel (a_v) = $0.0000051^\circ\text{C}^{-1}$

Temperature difference (dT) = 120°C

B = 0.0004 Mpa^{-1}

Batch diameter (D) = 8 cm

Batch thickness (t) = 2 cm

Elastic modulus of the vessel (E) = 193000 MPa

This pressure, equivalent to a water column of around 60 m, is not relevant for geothermal reservoirs, as the occurring pressure in greater depth could be higher but since most of the alteration processes are strongly controlled by temperature and only subsequently by pressure these errors are neglected.

6.4 Modeling

The possibility to perform chemical calculations comes from minimizing Gibbs free energy (G) applied to one or more species (i) in a closed system with constant pressure and temperature using the Chemical potential μ which relates changes in G with changes in the number of moles in solution (n_i):

$$\mu_i = \frac{\delta G_i}{\delta n_i}$$

For a species i the chemical potential will be:

$$\mu_i = \mu_i^\circ + RT_K \ln a_i$$

where μ_i° is the standard chemical potential, R is the gas constant, T_K is the temperature in kelvin and a_i is the activity of the species. Then, using the definition for the equilibrium constant of a reaction:

$$\ln K = -\frac{\Delta G^\circ}{RT_K}$$

it is possible to predict the value of the ionic activity product of a reaction at equilibrium using the mass action law:

$$K = \frac{\prod a_j^{n_j}}{\prod a_k^{n_k}}$$

where each product j has a mole number n_j and an activity a_j and each reactant k has mole number n_k and an activity a_k .

So to determine the equilibrium state of a system, it is necessary to have a thermodynamic database with the equilibrium constants of all the reactions taking place in the system at the specified temperature.

The software used for the water-rock interaction geochemical modeling and thermodynamic calculations was USGS Phreeqc 3.1.4 (Charlton & Parkhurst, 2011; Parkhurst & Appelo, 2013) and thermodynamic database used was `l1n1.dat` (by Lawrence Livermore National Laboratory) provided in the software. This software allows predicting the reactions that will occur for a given set of solid phases present in the rock. For the sake of simplicity, only equilibrium models were performed, in order to analyze a variety of rock samples in the development time considered for this work.

Since the software will only equilibrate phases that are specifically given as an input, it is necessary to determine, beforehand, the stable phases. Table 2 shows a list of phases stable under the estimated reservoir conditions and were therefore considered as possible alteration products for the modelling.

To be able to compare the modeling results with the batch reactor results, the mass proportion between water and rock is the same as in the experiments (water to rock proportion is ~3:1). The resulting composition is plotted against the thermal and meteoric water of the studied area.

Initial water composition for the modeling was not pure water, since meteoric waters provided better results compared to the hot spring water samples in the area. Although the difference might be irrelevant for most modeled elements, it did make a difference when the availability of a certain element was in the limit of producing a discrete change in the results. This can be appreciated in the discussion (item 8.3.1) where different initial water compositions produce almost the same results with exception of Mg which has a significant decrease in the pure initial water modelling.

In addition, stability diagrams and activity calculations were performed with the Student Edition of Geochemist's Workbench. These diagrams are explained in detail further in the methodology.

Table 2: list of stable minerals at reservoir and experiments conditions according to (Browne, 1978; Hellevang et al., 2013; Kristmannsdottir, 1979; Lagat, 2010; Reyes, 1990). Minimum and maximum temperatures represent the ranges of mineral stability. Temperatures in parenthesis mean that the mineral is not always present.

	Minimum T [°C]	Maximum T [°C]	Reference
Chlorite	20 ³ - 120 ^{1,2}	>200 ^{1,2,3}	1: Reyes 1990 (Neutral pH), 2: Lagat 2010, 3: Hellevang et al 2013
Laumontite	100 ¹ - 120 ^{2,3}	180 ² - 200 ¹ - 220 ³	1: Browne 1978, 2: Kristmannsdottir 1979, 3: Reyes 1990 (Neutral pH)
Calcite	20	-	Reyes 1990 (Neutral pH)
Dolomite	20	180	Reyes 1990 (Neutral pH)
Pyrite	20	-	Reyes 1990 (Neutral pH)
Smectites	20 ^{1,2,3}	200 ^{1,2}	1: Kristmannsdottir 1979, 2: Reyes 1990 (Neutral pH), 3: Hellevang et al 2013
Nontronite (Smec)	20	-	Hellevang et al 2013
Montmorillonite (Smec)	20	-	Hellevang et al 2013
Saponite (Smec)	50	-	Hellevang et al 2013
Wairakite (Zeo)	100	200	Browne 1978 (Neutral pH)
Quartz	100	200	Browne 1978 (Neutral pH)
Chalcedony	-	180	Lagat 2010
Mordenite (Zeo)	100	200	Lagat 2010
Illite	(120) - 200	-	Lagat 2010

6.4.1 Solid solutions thermodynamics in the Phreeqc models

Since there is limited thermodynamic data available for solid solutions, they were replaced by their end members in the same proportion as the SS mineral. For example, if after petrographic analysis and mass balance on a sample it is determined that there should be 1 mole of Na and 2 moles of Ca in plagioclases, then 1 mole of albite and 2 moles of anorthite are used for the modeling instead of 3 moles of labradorite.

6.4.2 Glass thermodynamics

As some of the rock samples have volcanic glass on them, it was necessary to determine the solubility equilibrium constants for the glass at various temperatures. To do so, a SEM FEI Quanta 250 with EDS (CEGA, Chile) was used to obtain glass compositions of the rocks used in the modeling (if required).

After, stability constants ($\log K$) values for glass were obtained using a similar method to the one proposed by (Paul, 1977) and also used in (Advocat et al., 1997; Aradóttir, Sonnenthal, & Jónsson, 2012; Bourcier et al., 1992; Leturcq, Berger, Advocat, & Vernaz, 1999; Techer, Advocat, Lancelot, & Liotard, 2001) which considers glass as an ideal solid solution between all the oxides that compose it.

This method might not be as accurate as experimentally analyzing the stability of glasses with these compositions, nevertheless, while this would definitely affect the results of a kinetic geochemical model, since this is an equilibrium model and no kinetic considerations are taken into account, at the given conditions, the glass phases are always completely dissolved.

In the end, glass $\log(K)$ value for a given temperature where the molar fractions (X_i) and solubility products (K_i) for each oxide are known, is defined as:

$$\log K_{glass} = \sum_i X_i \log K_i + \sum_i X_i \log X_i$$

If the solubility products are known for at least 6 different (well distributed) temperatures, then it is possible to generate an analytical expression for the glass solubility constant by replacing it in the following equation and obtaining all 6 a_i constants:

$$\log K_{glass} = a_1 + a_2 T + \frac{a_3}{T} + a_4 \log T + \frac{a_5}{T^2} + a_6 T^2$$

Finally, this analytical expression can be attached to any Phreeqc thermodynamic database.

A Matlab code used to obtain stability constants for glass can be found in the appendix 11.4. Thermodynamic input data used was obtained from (Aradóttir et al., 2012).

6.4.3 Modeling alteration phases

In order to get the most probable alteration minerals for simulated water-rock interaction of selected samples, at first they were tested using all possible alteration minerals displayed in table 2 and then the ones that failed to predict the thermal water composition were left out. Also, some of the initial solid phases present in the rock such as pyroxenes, amphiboles, anorthite and other rock forming minerals were forced to dissolve only.

6.4.4 Activity diagrams

Using the student edition of Geochemist's Workbench software, activity vs activity (log activity ratios) diagrams were made. In these diagrams the fluid chemistry of thermal waters, batch reactor results and Phreeqc results were plotted. To do so, the activities of the selected cations were calculated using the GSS tool and then they were plotted in diagrams displaying Al species stability using the Act2 tool.

These graphs are very useful as they allow comparing the different experimental approaches used in this work with the measured thermal water compositions, permitting, as well, visualizing the evolution of the batch reactor experiments in time in order to evaluate the consistency of the results. Also, comparing activities is more accurate in terms of evaluating water rock interaction results. All stability diagrams suppose an equilibrium with quartz ($\text{SiO}_2(\text{aq})$) and feldspar (Al^{+++}).

6.5 Nomenclature

A small clarification has to be made in order to understand the nomenclature used for samples, experiments and models. While rock samples have a name such as "IV-4" the resulting water of an alteration experiment using sample IV-4 will have a name such as "exp(IV-4)" and consequently, the resulting water of a geochemical model using sample IV-4 as the reacting rock is named as "mod(IV-4)".

7 Results

7.1 Mineralogy

Detailed results for outcrop, hand sample and thin section descriptions and interpretations can be found on the appendix 11.1 and 11.2. XRD results can also be found in the appendix 11.3. Rock sample, thin section and XRD mineralogy description is summarized in table 3.

As shown in table 3, although all samples are composed of volcanic material, 4 out of 9 samples are clastic sedimentary rocks (IV-1, IV-7, IV-8 and IV-11), 1 is a pyroclastic deposit (IV-5) and 4 are plain volcanic rocks (IV-4, IV-6, IV-9 and IV-10) which range from basaltic andesites to dacites.

7.2 SEM-EDS

Results for SEM-EDS analysis of glass compositions in samples IV-5 (pyroclastic) and IV-6 (lava) are presented in tables 4 and 5 respectively.

4 points were analyzed where glass was believed to be present (by optical microscope interpretations). In both samples, the most divergent point was left out.

Table 3: Glass composition obtained from SEM-EDS of sample IV-5, discarded spectrums are in red.

Spectrum	Na2O (%)	MgO (%)	Al2O3 (%)	SiO2 (%)	K2O (%)	CaO (%)	TiO2 (%)	Fe2O3 (%)
1	2.85	1.09	12.96	35.21	2.89	22.27	2.22	20.51
2	2.02	0.76	14.48	32.54	5.63	20.14	1.47	22.96
3	2.53	4.23	18.25	42.45	0.57	19.81	0.92	11.24
4	1.50		26.41	39.34		29.97		2.78

Table 4: Glass composition obtained from SEM-EDS of sample IV-6, discarded spectrums are in red.

Spectrum	Na2O (%)	MgO (%)	Al2O3 (%)	SiO2 (%)	K2O (%)	CaO (%)	TiO2 (%)	Fe2O3 (%)
1	10.56	0.00	12.52	74.32	0.00	2.08	0.00	0.51
2	2.93	0.00	3.71	88.34	0.26	3.00	0.36	1.40
3	15.03	0.86	20.81	55.53	0.29	3.08	0.00	4.39
4	3.60		4.82	90.38		0.70		0.50

Table 5: Sample description made with hand sample, petrographic microscope and XRD analysis.

Sample	E	N	Description	Primary minerals	Secondary minerals	Volcanic glass %
IV-1	746846	5635397	Fine grain gray sandstones with varves intercalated with mid grain sandstones with ondulites	Quartz (20%), K-feld (10%), Plagioclase (30%), Opaques (Fe-Ox) (15%), hornblende (10%), Olivine-Mg-Fe (5%), Pyroxene-Al-Fe-Mg (5%), montmorillonite (5%)		0%
IV-4	275719	5636592	Porphyric basaltic andesite with clinopyroxene, abundant lithics	Plagioclase Ca-Na (40%), Clinopyroxene Mg-Fe-Ca (30%), Magnetite (10%)	Chlorite(5%): clinochlore & chamosite, Chalcedony-SiO2 (5%), Clay (10%): greenalite & Kaolinite	0%
IV-5	277494	5642420	Pyroclastic or lahar deposit with coarse grain ash matrix (60%) and polymictic volcanic and intrusive clasts from 5 mm to 1 m	Plagioclase (60%), Olivine Fe-Mg (10%), Pyroxene Mg-Ca-Zn (15%)	Iddingsite (<5%), Chlorite (<5%), Fe-Ox (10%)	30%
IV-6	275814	5641539	Porphyric dacite with biotite	Quartz (20%), Plagioclase (30%), Biotite (<5%), Titanomagnetite (15%)	Clay (15%), Chlorite: (10%), Epidote (10%), Actinolite (<5%)	20%
IV-7	272054	5655008	Volcano-clastic conglomerate. Mid grain green and purple matrix (25%), clasts are polymictic, volcanic, rounded and angular. It presents red veins of 5-10 cm thick, and chloritization of matrix	Plagioclase (5%), Quartz (65%)	Calcite (20%), Fe-Ox: Hematite (5%) & Magnetite (<5%), Zeolite (<5%)	Glass was present but is completely altered
IV-8	249493	5668924	Thick volcano-sedimentary monomictic conglomerate	Plagioclase (50), Pyroxene (5%), Olivine (5%), Muscovite (<5%), Magnetite (5%), Quartz (5%), Hornblende (<5%)	Chlorite (10%): Clinochlore & Chamosite, Calcite (15%)	0%
IV-9	251039	5666865	Porphyric Andesite with pyroxene	Plagioclase (40%), Clinopyroxene (10%), Titanomagnetite (15%)	Chlorite (5): clinochlore & chamosite, Clay: greenalite (20%), Calcite (5), Quartz (5%)	Glass was present but is completely altered
IV-10	250134	5666362	Porphydic andecite with 2-20 mm elongated horizontal amygdales filled with calcite and quartz	Plagioclase (60%), Magnetite (10%)	Chlorite (10%), Clay (5%), Quartz (5%), Calcite (10%)	0%
IV-11	249763	5666297	Very finely stratified deposit	Quartz (45%), Albite (45%)	Chlorite (10%): clinochlore & Chamosite	0%

7.3 XRF

Table 6: bulk composition for selected samples using XRF

Sample	Na2O (%)	MgO (%)	Al2O3 (%)	SiO2 (%)	P2O5 (%)	K2O (%)	CaO (%)	TiO2 (%)	MnO (%)	Fe2O3 (%)
IV-4	2.49	4.66	17.23	54.56	0.22	1.51	8.10	0.96	0.14	7.84
IV-5	2.98	4.27	17.78	51.99	0.33	1.18	8.24	1.24	0.17	9.45
IV-6	3.64	0.94	14.02	71.30	0.09	4.07	1.93	0.40	0.07	2.48
IV-7	3.18	1.53	14.10	64.90	0.15	1.89	4.06	0.60	0.10	4.26
IV-8	3.86	5.02	18.99	49.67	0.27	0.78	6.37	1.31	0.11	9.48

7.4 Mass balance

Table 7 displays the resulting mineralogy after performing the mass balance comparing the mineralogy obtained by petrographic microscope and X ray diffraction with the bulk rock composition obtained by X ray fluorescence. Some important changes can be seen in solid solutions and Fe bearing minerals.

Table 7: Mineral percentages obtained by microscope analysis (i) and after mass balance (f)

Phase	Formula	IV4i	IV4f	IV5i	IV5f	IV6i	IV6f	IV8i	IV8f
Albite	NaAlSi3O8	19	22	30	21	14.25	5	23.75	36
K-feld	KAlSi3O8	2	9.2	5	5	1.5	24	2.5	0.5
Anorthite	CaAl2Si2O8	19	18	30	23	14.25	3	23.75	14.5
Magnetite	Fe3O4	10	7			15	1	5	1
Greenalite (clay)	Fe3Si2O5(OH)4	5	0			7.5			
Kaolinite	Al2Si2O5(OH)4	5	10			7.5	2		
Qtz/Chalc	SiO2	5	10	0	12	20	39	5	10
Clinochlre-14A	Mg5Al2Si3O10(OH)8	2.5	4.8			10	2	5	8
Chamosite-7A	Fe2Al2SiO5(OH)4	2.5	0					5	10
Diopside	CaMgSi2O6	15	15	7.5	6.5			2.5	1
hedenbergite	CaFeSi2O6	15	4	7.5	0			2.5	3
Hematite	Fe2O3			10	1				
Forsterite	Mg2SiO4			5	5.2			2.5	3
Ferrosilite	Fe2SiO4			5	6.3			2.5	4
Epidote	Ca2FeAl2Si3O12OH					10	4		
Calcite	CaCO3							15	3
Muscovite	KAl3Si3O10(OH)2							5	6
glass iv5	SiAl10.415Fe0.213Mg0.075Ca0.385Na0.085K0.034O3.355			30	20				
glass iv6	SiAl10.39Fe0.04Mg0.018Ca0.0389Na0.331K0.004O2.8494					20	20		

7.5 Alteration experiments: exp(IV-4)

A summary of the results is presented in table 8. Also, evolution of some elements is presented in figure 10.

As seen in the trend of most elements in figure 10, the steady state (full equilibrium) has not yet been reached at 90 days but while not it might not be completely steady, there is very little difference between 120 and 180 days experiments; also, 10 and 60 days experiments (dashed lines in figure 10) greatly differs from the rest of the samples in Cl and K content.

Also, at the beginning, some elements behave rather randomly. More debate can be found in the discussion section.

Table 8: Selected elements and physicochemical parameters present in resulting waters from batch experiments using sample IV-4 (exp(IV-4)).

Time	Na	Mg	Al	K	Ca	Si	Li	Rb	B	Sr	As
Days	mg/l	mg/l	ug/l	mg/l	mg/l	mmol/l	ug/l	ug/l	ug/l	ug/l	ug/l
10	79.44	0.114	480.2	51.51	11.91	1.31	6.132	34.14	50.84	75.24	9.782
20	87.33	0.076	348.8	18.75	11.242	1.38	7.202	23.9	50.9	77.58	8.864
30	90.7	0.058	472.4	13.816	9.346	1.21	7.18	24.12	51.32	65.32	8.838
45	96.58	0.14	221	16.174	16.162	1.88	9.332	17.334	56.34	138.18	7.112
60	99.06	0.14	366	74.86	10.176	1.82	10.462	22.48	56.68	99.12	8.472
90	111.32	0.188	211.35	13.83	14.444	1.88	15.392	20.44	61.17	142.77	7.03
120	108.26	0.082	209.4	7.046	10.51	1.81	11.86	16.554	67.86	100.08	7.448
180	118.24	0.087	266.82	5.958	9.936	1.76	12.838	14.314	64.08	84.36	7.323

Time	F	Cl	S	pH	HCO3-	CO32-	Total Carbonate
Days	mg/l	mg/l	mg/l		mmol/l	mmol/l	mmol/l
10	0.231	66.9	8.74	8.5	2.5	0.2	2.7
20	0.444	42.9	10.28	8.52	1.9	0.4	2.3
30	0.334	40.6	8.76	8.52	2.6	0.25	2.85
45	0.416	46.8	15.04	8.45	2.8	0.2	3
60	0.463	99.7	9.89	8.25	3.4	0	3.4
90	0.748	55.5	14.03	8.25	3.6	0	3.6
120	1.846	41.1	27.59	8.3	2.9	0.2	3.1
180	1.711	38.99	34.66	8.43	2.8	0.4	3.2

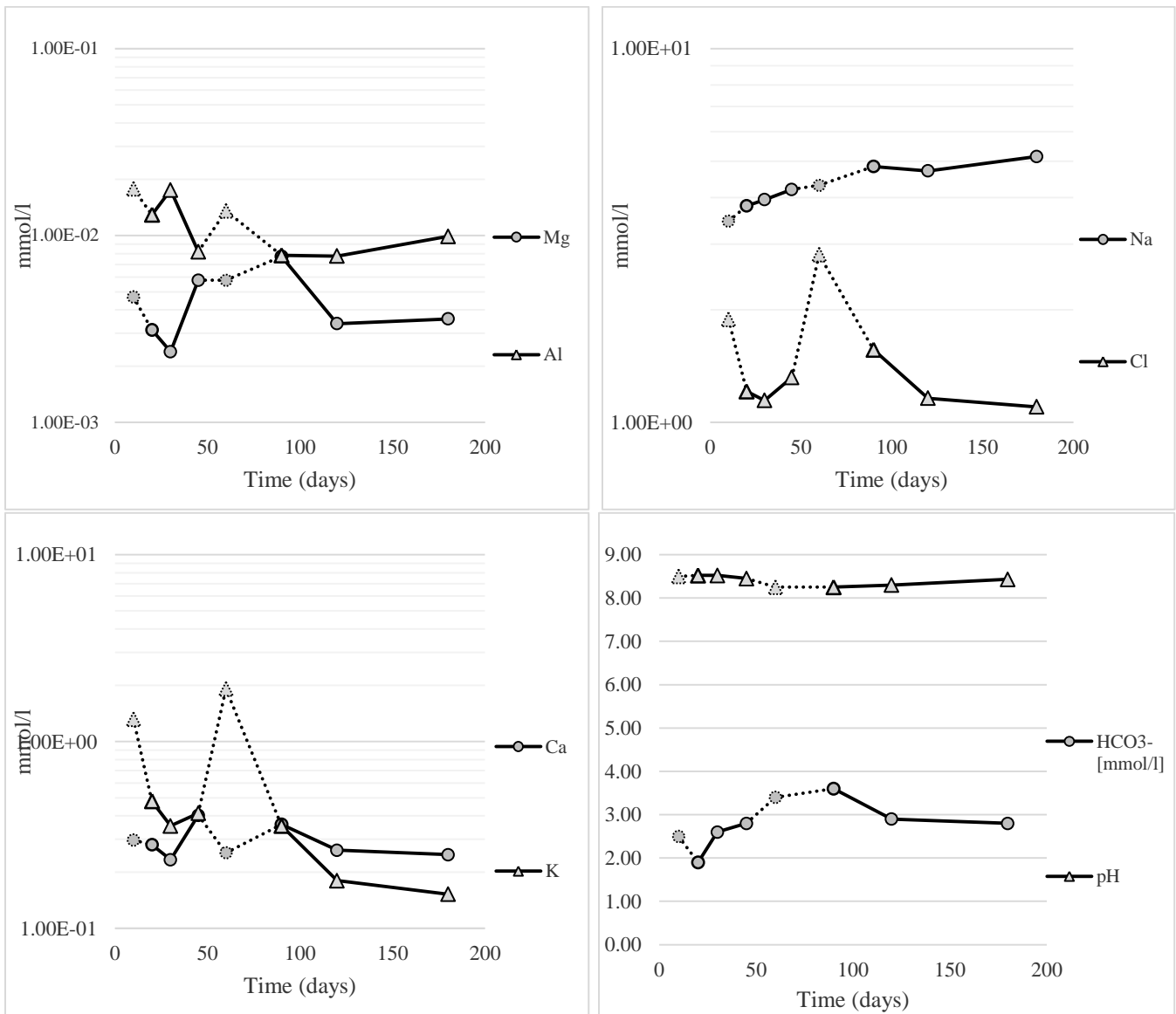


Figure 10: The evolution of Mg, Al, Na, Cl, Ca, K, HCO₃⁻ and pH in the batch reactor experiments for the selected sample IV-4. Unsuccessful experiments (10 and 60 days) are plotted using dashed lines.

7.6 Modeling

Input alteration phases provided to achieve modeling results were selected from the list of possible stable phases listed in the methodology, but the ones producing the best fitting results were used: IV-4: Kaolinite, Nontronite, Mordenite; IV-5: Saponite, Prehnite; IV-6: Montmorillonite, Nontronite, Saponite

& IV-8: Montmorillonite, Nontronite, Saponite. As well, it is worth mentioning that also cation exchange was allowed between K-feldspar and Albite.

Figure 11 summarizes the most important results. Colored lines show resulting water compositions of Phreeqc water-rock interaction models for samples IV-4, IV-5, IV-6 and IV-8 and the long term batch reactor experiment (90 days). In contrast, natural thermal water compositions are plotted in black lines for Panqui, Toledo, Menetue and Los Pozones hot springs. Given the high composition variance found on the natural thermal waters, a logarithmic scale was believed to be the best way to compare the different results obtained by the experimental methodologies.

What can be seen from the figure 11 is that, in most cases, Phreeqc models results deviate strongly to the Mg and Fe contents compared to the spring waters and the batch reactor fluids, with the exception of sample IV-4 which is the one with the best fitting Fe content and it shows exactly the expected Mg content. Consequently this sample was the one used for the batch reactor experiments. Also, Na, K, Ca and Si contents fit to the expected values, except for sample IV-5 which was the most discrepant to the natural thermal waters from the area.

Detailed input data for the Phreeqc modelling can be found on the appendix 11.5.

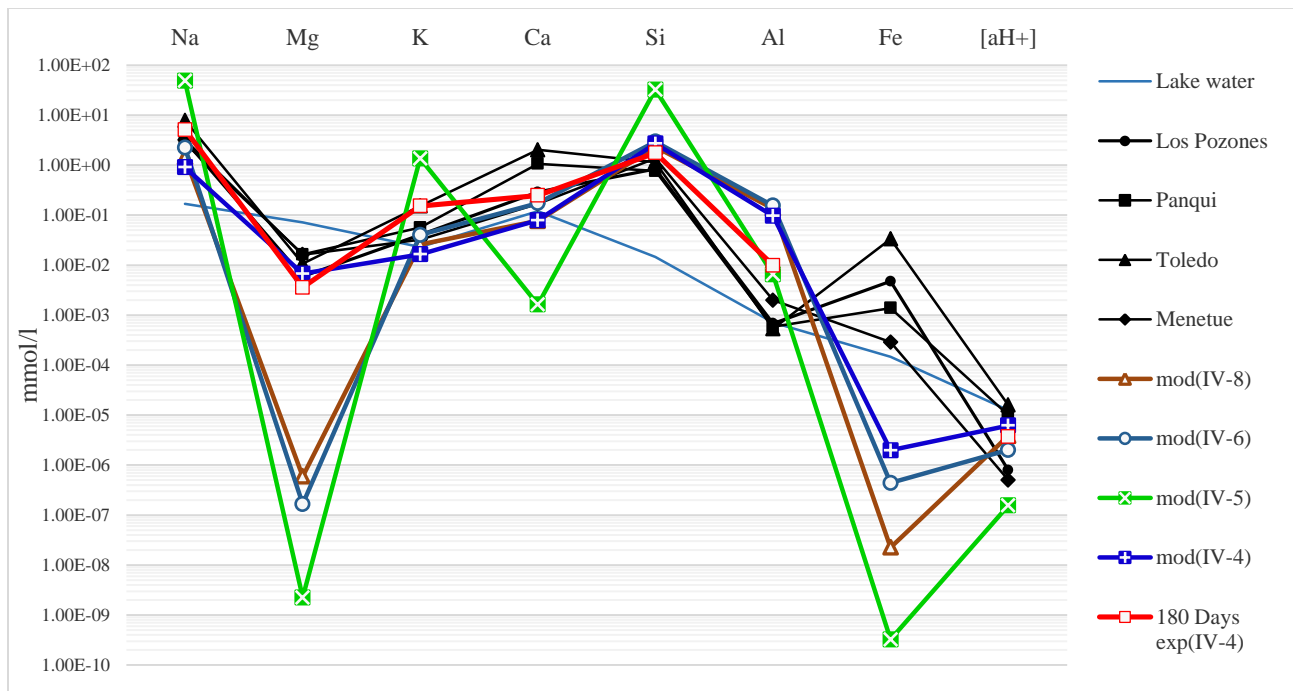


Figure 11: Concentrations in mmol/L of cations and H⁺ activities in thermal waters (Pangui, Toledo, Menetue, Los Pozones), peripheral water samples (Villarrica Lake water), Phreeqc modeling results (IV-4, IV-5, IV-6 & IV-8) and a long term batch experiment (90 days).

8 Discussions

8.1 Petrography

8.1.1 Selected samples

Since only 1 sample could be selected for the batch reactor experiments, an important decision had to be made. First of all, all plain sedimentary clastic samples were left out because the majority of the outcrops of volcanic sedimentary units are either volcanic or volcanoclastic (such as pyroclastic). Then the proximity to thermal waters and degree of alteration was considered, leaving out the most altered samples. In the end, IV-4 was chosen as the one that best fitted to the required characteristics.

8.1.2 Mass balance

The resulting mineralogy after the mass balance was for most of the rocks and minerals somewhat similar to the original one, changing moderately the proportions between different minerals but changing significantly the proportions between solid solutions (Table 7). As well, the reduction of iron bearing minerals was quite significant. It is important to notice that the sample IV-5 which is considered a pyroclastic deposit could not be explained without a small amount of quartz. Probably, the matrix had sand and/or silt so it was not composed entirely of volcanic glass (ash) which made the quartz not distinguishable just by petrographic microscope. Finally, sample IV-6's feldspars had a significantly higher amount of K than what was believed just by microscope analysis.

8.2 Alteration experiments

8.2.1 Blank experiment

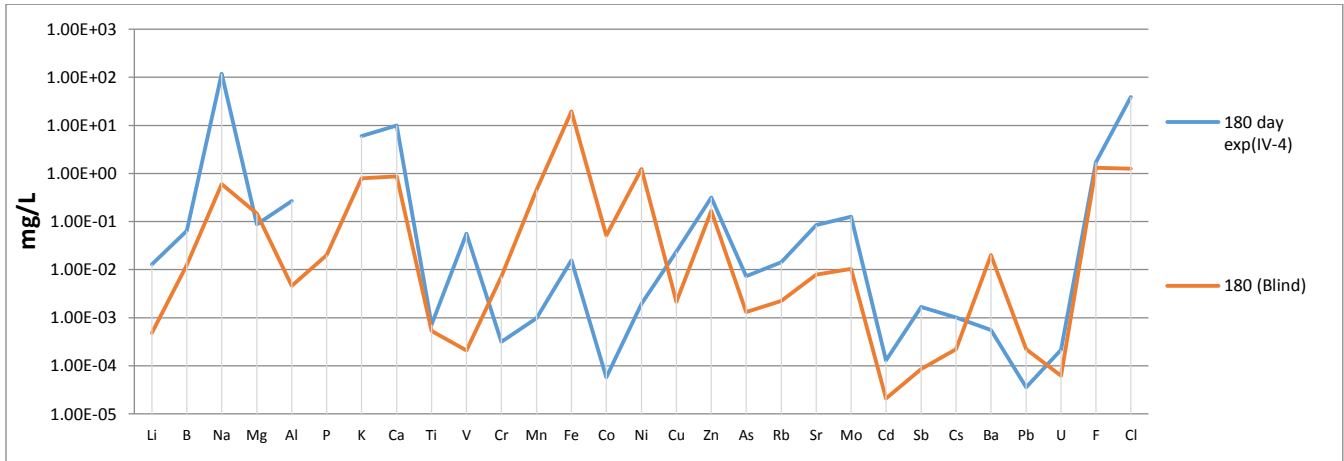


Figure 12: Concentration of measured elements in solution after 180 days in the alteration experiment with rock sample IV-4 and blind (only pure water).

Unfortunately, the blind experiment (pure water and no rock sample) conducted at 180 days has a considerable amount of dissolved elements (Figure 12). This is particularly high for all elements related to stainless steel alloys such as Cr, Mn, Fe, Co & Ni. Therefore, these elements are not to be used for any consideration or interpretation since it is not possible to differentiate if their concentration is a consequence of this corrosion or the water-rock interaction.

The high amount of contamination is a severe problem for any interpretations made in this thesis since the ionic strength of the solution changes affecting also the elements that are not as high as Cr, Mn, Fe, Co and Ni. Therefore, the alteration experiments results should be used with caution.

8.2.2 Failed experiments

Not only the 10 and 60 days experiments behave notoriously different as seen in figure 10, but also do not follow the common trend in the temperatures given by geothermometers (figures 13 and 14) nor in the activity diagrams (figure 15). So it follows that these experiments might have had a failure during the experimental process. Therefore, these experiments should not be used for any consideration.

8.2.3 Limitations

In the batch experiments, only water rock interaction effects are taken in consideration so any process like magmatic input or different initial water compositions are neglected. That could lead to a thermodynamic equilibrium of the system much different from the real thermal waters in the studied area. Even though these are important limitations, it has the benefit of isolating the effects of water-rock interaction in the whole process.

Other limitation is that, on one hand, geochemical models only focus on major cations and on the other hand, batch reactor experiments have trace element contamination from the stainless steel vessels so in the end, the only important deductions that can be made from this work are those derived from major cations and physicochemical conditions, not to mention that with only that information as an input the interpretations are complicated enough for the scope of this work.

As well, since this work is encompassed in a larger project, it lacks the contrast with basement units which will be published by KIT researchers in the near future. If this contrast exists and there is a clear difference with the experiments from granitic samples then significant conclusions could be made about the units that control the fluid chemistry in the vicinity of Villarrica volcano.

8.2.4 Geothermometers and evolution of alteration experiments

As shown in figure 13, quartz geothermometer (R.O. Fournier & Potter, 1982) is the best fitting geothermometer for the alteration experiments performed with the selected sample (IV-4), whereas chalcedony (R.O. Fournier & Potter, 1982) delivers a much lower temperature. On the other hand, Na-K-Ca cation geothermometer (R O Fournier, 1981) completely fails to predict the temperature for the long term experiments.

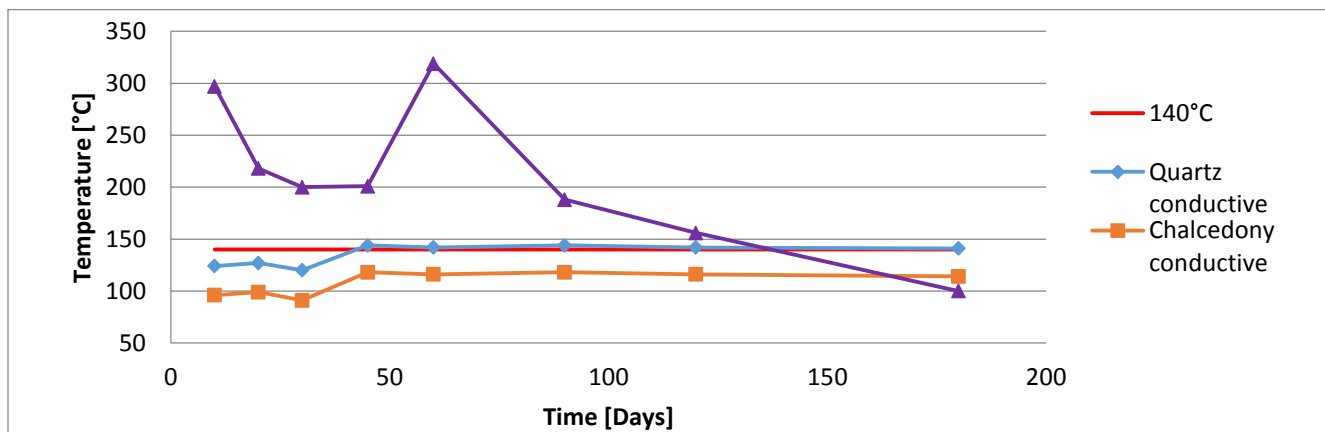


Figure 13: evolution in time of 3 geothermometers applied to the alteration experiment results. Silica reference: Fournier & Potter (1982). Cation reference: R O Fournier (1981).

In contrast, figure 14 shows the Na-K-Mg ternary diagram (Giggenbach, 1991) where it is possible to see that if “failed” experiments are left out (10 and 60 day experiments), the evolution of the system clearly is towards the equilibrium temperature (140°C), But even at 180 days this has not happened.

The intense variability in the evolution of some elements at the beginning of the alteration experiments can be the result of uneven depletion of elements in the process of mineral precipitation, which can lead to changes in the stability of phases that control the solubility of certain elements (Michard, 1991), in other words, if a mineral precipitation consumes A and B and the system runs out of B, then the solubility of A is suddenly controlled by another mineral phase which, in turn, could lead to an abrupt change in the dissolved content of A. Nevertheless, as discussed before, 10 and 60 day experiments probably had a failure in part of the experiment so their high values of Cl and K are a consequence of this.

In the same way, some of the activity/activity diagrams of figure 15 show a nice trend in the evolution of the system but both 10 and 60 day experiments do not. Yet, this linear evolution in the activity diagrams, together with the fact that the batch experiments and the Phreeqc models have similar activity ratios and are located most of the times in the same stability field, are features that somehow confirm the validity of the proposed methodology.

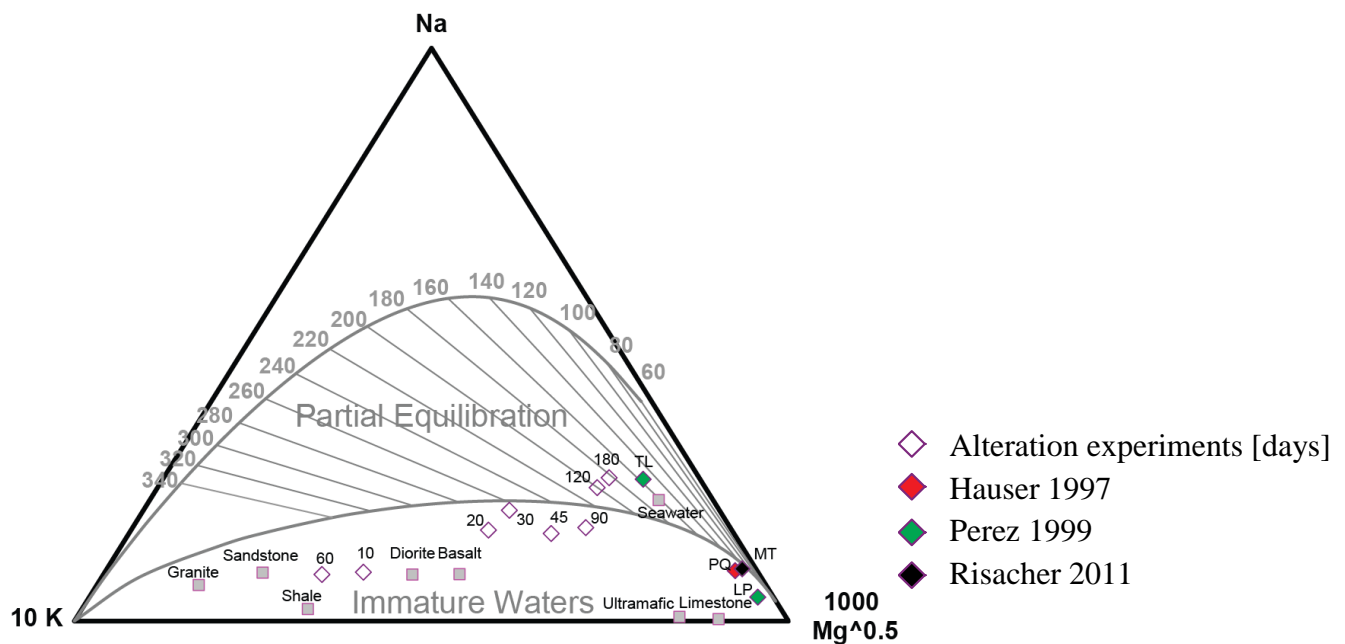


Figure 14: Na-K-Mg ternary diagram (Na-K and K-Mg geothermometers) displaying the alteration experiment water compositions and four hot spring samples.

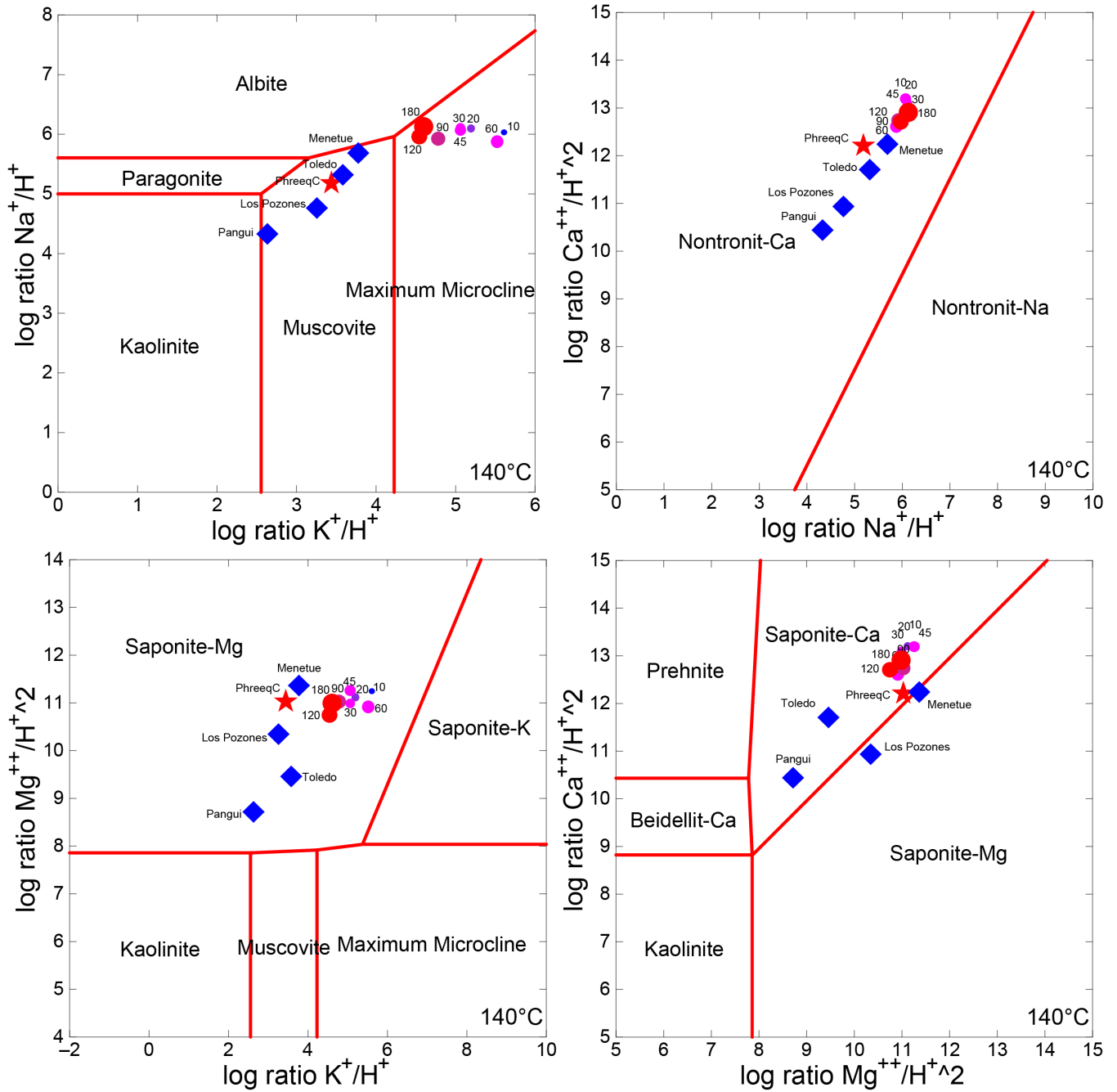


Figure 15: Activity vs Activity diagrams displaying Al species stabilities. Batch reactor, Phreeqc modeling and Los Pozones spring activities are plotted.

8.3 Analysis of boundary conditions sensitivity for geochemical models

With the purpose of quantifying the relevance of the different variables involved in the geochemical modeling, a sensitivity analysis was made for the following initial conditions: water composition, pH, PE and rock/water proportion.

8.3.1 Initial water composition

Figure 16 shows the Phreeqc results for the interaction between different initial waters and rock sample IV-4, as can be appreciated in the graph, pure water as initial condition only affects the behavior of Mg. Nevertheless, since there seems to be a 10% mixing with peripheral waters (personal communications with Held, S. January 2015), the resulting mix should have a similar Mg content as in the other initial water compositions so thermal water samples would not actually reflect this low Mg content.

8.3.2 pH

From figure 17 it is clear that initial pH condition is one of the most sensitive variables for the geochemical modeling. Extreme pH values as 1 and 10 give results far from being close to Menetue hot spring, but for intermediate values such as 3 and 7 this difference is a bit lower. For most cations, lower pH results in higher rock leaching. This means that if acid steam heated waters interact with the rock units, the resulting thermal water composition would differ greatly from a neutral water interaction.

8.3.3 Initial p ϵ conditions

Highly reducing initial conditions affect Fe and Mg, as can be seen in figure 18. A p ϵ value of -8 would be equivalent to a EH of approximately -650 mV which is near the limit of water stability field at this pH conditions which is probably not the best guess for the initial water conditions, assuming this water has a meteoric origin so this supports the use of a slightly oxidized conditions for the initial water.

8.3.4 Final p ϵ conditions

By fixing final p ϵ conditions, the value is not a result of redox equilibrium; therefore, it will probably not resemble a natural process, but for the sake of understanding the importance of this parameter, a sensitivity analysis was done. The results (Figure 19) show that for higher redox potentials, lower concentrations of Fe stay in solution. Also the redox potential affects Al, Ca and in a lesser extent, all other elements in the figure. This might be explained not only by direct consequence of redox potential,

but also by changes in the saturation indexes due to higher depletion of elements used in Fe bearing minerals.

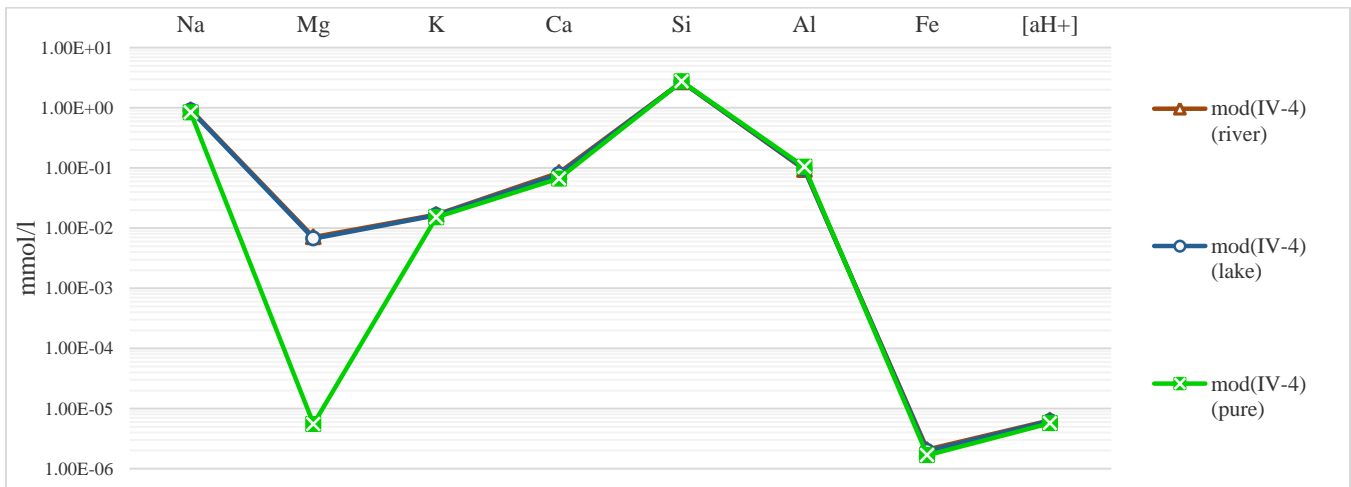


Figure 16: Phreeqc results for IV-4 with different initial water composition

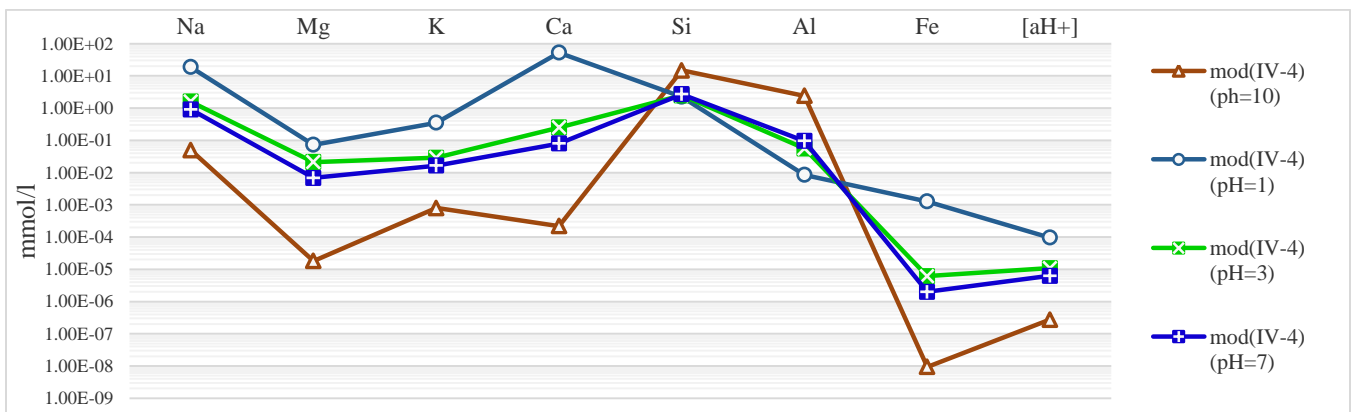


Figure 17: Phreeqc results for IV-4 with different initial pH values

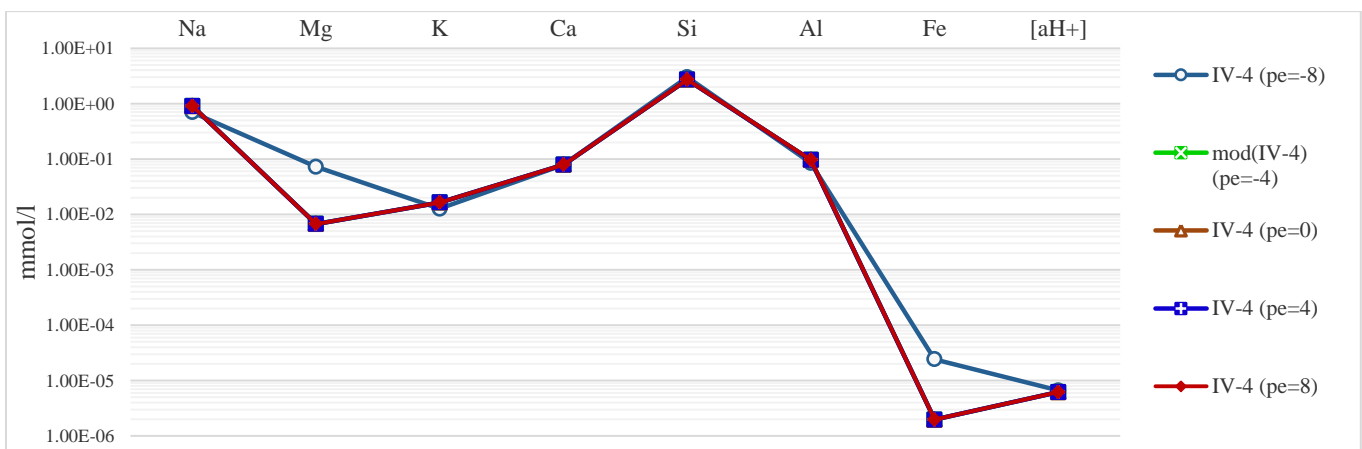


Figure 18: Phreeqc results for IV-4 with different initial pe values

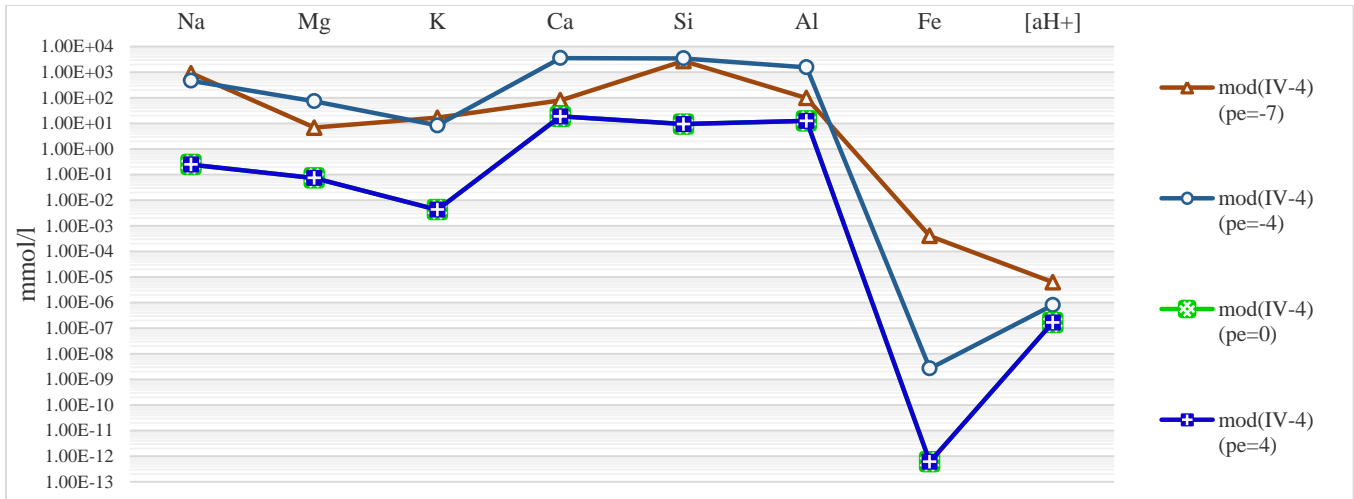


Figure 19: Phreeqc results for IV-4 with different fixed final pe values

8.4 A general overview of the results: comparison between batch reactor experiments, modeling results and thermal waters in the area

Figure 11 compares the results of the batch reactor experiments, the results of the Phreeqc modeling and the thermal waters in the area. This graph shows a nice similarity between the cation concentrations found in the thermal waters, the IV-4 sample batch experiment, and the geochemical models for samples IV-4, IV-6 and IV-8, only sample IV-5 displays an important deviation in the resulting water composition. It is particularly interesting the remarkable match between the 90-days-experiment and the natural water composition, which stands as one of the most important results of this work, since serves to accomplish one of the most important objectives initially proposed.

The most important consequence is that probably the solubility of the plotted cations in all these waters are controlled by the mineral phases proposed in the methodology, in other words, the interaction between the volcanosedimentary units of the Villarrica area and thermal waters at 140°C could explain the concentrations of certain cations in this area.

Furthermore, the hypothesis that heat-water-rock interaction processes between geothermal waters and volcanic or volcano-sedimentary units are relevant factors controlling the chemistry of thermal waters north of Villarrica volcano was, to a certain degree, tested using alteration experiments and thermodynamic simulations and this methodology was successful in predicting the behavior of the natural system.

9 Conclusions

To really assess the relevance of the results it is important to take into consideration all the limitations and consequences of the elected methodology. Both geochemical models and alteration experiments are a good approach to understand natural systems, such as hydrothermal systems, but they oversimplify reality. In particular, the thermodynamic equilibrium models, or simple equilibrium models (Bethke, 2008), and batch reactor experiments do not consider reaction kinetics, nor the heterogeneity of the system in terms of composition, permeability or physicochemical conditions. Chemical heterogeneity is a major problem since the results are limited to a very few rock samples. So any kind of result obtained by this should be regarded as a general approximation.

Likewise, the hydrothermal systems north of Villarrica volcano could be controlled by many processes other than heat-water-rock interaction, which are not taken into account in this work in order to solely assess the relevance of heat-water-rock interaction processes in the chemistry of thermal waters in the area, and this, applied only to volcanic and volcanoclastic units.

That said, experimental work in this thesis has shown the applicability of the proposed methodology to a better understanding of the heat-water-rock interactions in active geothermal systems. Moreover, in spite of the limited number of samples used and the reduced number of elements analyzed, with the results it is possible to predict the behavior of rocks that could act as reservoir in the geothermal systems near the Villarrica volcano (Figure 11), specifically, that heat water rock interaction processes between geothermal waters and volcanic or volcano-sedimentary units are relevant factors controlling the chemistry of thermal waters in the area. This is especially relevant for future exploration as it may guide the initial efforts to find middle enthalpy reservoirs.

Also, the application of this methodology to the other main geological units in the area should help to clear up the relevance of the volcano-sedimentary units in the geothermal systems in the area, with the possibility to enhance the considerations taken into account in order to assess not only the relevance of heat-water-rock interaction processes but also other processes such as cooling, mixing or input of acid magmatic fluids.

10 Bibliography

- Advocat, T., Chouchan, J. L., Crovisier, J. L., Guy, C., Daux, V., Jegou, C., ... Vernaz, E. (1997). Borosilicate Nuclear Waste Glass Alteration Kinetics: Chemical Inhibition and Affinity Control. *MRS Proceedings*, 506(August 2015). <http://doi.org/10.1557/PROC-506-63>
- Anderson, G. M. (2009). *Thermodynamics of Natural Systems*. Cambridge University Press.
- Aradóttir, E. S. P., Sonnenthal, E. L., & Jónsson, H. (2012). Development and evaluation of a thermodynamic dataset for phases of interest in CO₂ mineral sequestration in basaltic rocks. *Chemical Geology*, 304-305, 26–38. <http://doi.org/10.1016/j.chemgeo.2012.01.031>
- Aravena, D. (2014). Balance volumétrico comparativo de edificios volcánicos en la Zona Volcánica Sur. In *Jornada de postgrado del Departamento de Geología de la Universidad de Chile*. Santiago, Chile.
- Asturias, F. A. (2012). Status update of geothermal development in Guatemala. Presented at “short Course on Geothermal Developments and Geothermal Wells”. El Salvador.
- Bastrakov, E. N., & Shvarov, Y. V. (2007). HCh for Windows - a software package for geochemical equilibrium modelling. Geoscience Australia.
- Benjamin, T., Charles, R., & Vidale, R. (1983). Thermodynamic parameters and experimental data for the Na-K-Ca geothermometer. *Journal of Volcanology and Geothermal Research*, 15(1-3), 167–186. [http://doi.org/10.1016/0377-0273\(83\)90099-9](http://doi.org/10.1016/0377-0273(83)90099-9)
- Bethke, C. M. (2008). *Geochemical and Biochemical Reaction Modeling*. Cambridge University Press (Second Edi). Cambridge.
- Bethke, C. M., & Yeakel, S. (2015). *GWB Essentials Guide*. Aqueous Solutions, LLC Champaign, Illinois.
- Bourcier, W., Weed, H. C., Nguyen, S. N., Nielson, J. K., Morgan, L., Newton, L., & Knauss, K. G. (1992). Solution compositional effects on dissolution kinetics of borosilicate glass. In Y. Kharaka, A. Maest (Eds.), *WRI-7 Symposium Proceedings* (pp. 81–84). Balkema, Rotterdam.
- Brantley, S. L., & Chen, Y. (1995). Chemical weathering rates of pyroxenes and amphiboles. *Reviews in Mineralogy and Geochemistry*, 31(1), 119–172.
- Browne, P. R. L. (1978). Hydrothermal alteration in active geothermal fields. *Annual Review of Earth and Planetary Sciences*, 6, 229–250.
- Cembrano, J., & Lara, L. (2009). The link between volcanism and tectonics in the southern volcanic zone of the Chilean Andes: A review. *Tectonophysics*, 471(1-2), 96–113. <http://doi.org/10.1016/j.tecto.2009.02.038>
- Charlton, S. R., & Parkhurst, D. L. (2011). Modules based on the geochemical model PHREEQC for use in scripting and programming languages. *Computers & Geosciences*, 37(10), 1653–1663. <http://doi.org/10.1016/j.cageo.2011.02.005>
- DGA (Dirección General de Aguas). (1987). *Balance hídrico de Chile*.
- Díaz-González, L., Santoyo, E., & Reyes-Reyes, J. (2008). Tres nuevos geotermómetros mejorados de Na / K usando herramientas computacionales y geoquimiométricas : aplicación a la predicción de temperaturas de sistemas geotérmicos. *Revista Mexicana de Ciencias Geológicas*, 25(3), 465–482.
- Dickson, F. W., & Potter, J. M. (1982). *Rock-brine chemical interactions. Final report*. Stanford, California.
- Ellis, A. J. (1968). Natural hydrothermal systems and experimental hot-water/rock interaction: Reactions with NaCl solutions and trace metal extraction. *Geochimica et Cosmochimica Acta*, 32(12), 1356–1363.

- Ellis, A. J., & Mahon, W. A. J. (1967). Natural hydrothermal systems and experimental hot water/rock interactions (Part II). *Geochimica et Cosmochimica Acta*, 31(4), 519–538. [http://doi.org/10.1016/0016-7037\(67\)90032-4](http://doi.org/10.1016/0016-7037(67)90032-4)
- Eriksson, G., Hack, K., & Petersen, S. (1997). ChemApp - A programmable thermodynamic calculation interface. In *Werkstoffwoche '96, Symposium 8 Simulation, Modellierung, Informationssysteme*. Frankfurt, Germany: DGM Informationsgesellschaft mbH.
- Fournier, R. O. (1981). Application of water geochemistry to geothermal exploration and reservoir engineering. *Geothermal Systems: Principles and Case Histories*, 113.
- Fournier, R. O., & Potter, R. W. I. I. (1982). Revised and expanded silica (quartz) geothermometer. *Bull., Geotherm. Resour. Counc. (Davis, Calif.); (United States)*, 11:10.
- Fournier, R. O., & Truesdell, A. H. (1973). An empirical Na-K-Ca geothermometer for natural waters. *Geochimica et Cosmochimica Acta*, 37(5), 1255–1275. [http://doi.org/10.1016/0016-7037\(73\)90060-4](http://doi.org/10.1016/0016-7037(73)90060-4)
- Giggenbach, W. F. (1991). Chemical techniques in geothermal exploration. In *Application of geochemistry in resources development* (pp. 119–144). UNITAR/UNDP Guidebook.
- Gislason, S. R., & Eugster, H. P. (1987). Meteoric water-basalt interactions. II: A field study in N.E. Iceland. *Geochimica et Cosmochimica Acta*, 51(10), 2841–2855. [http://doi.org/10.1016/0016-7037\(87\)90162-1](http://doi.org/10.1016/0016-7037(87)90162-1)
- Gislason, S. R., Veblen, D. R., & Livi, K. J. T. (1993). Experimental meteoric water-basalt interactions: Characterization and interpretation of alteration products. *Geochimica et Cosmochimica Acta*, 57(7), 1459–1471. [http://doi.org/10.1016/0016-7037\(93\)90006-1](http://doi.org/10.1016/0016-7037(93)90006-1)
- Hajash, A., & Archer, P. (1980). Experimental seawater/basalt interactions: Effects of cooling. *Contributions to Mineralogy and Petrology*, 75(1), 1–13. <http://doi.org/10.1007/BF00371884>
- Hauser Y., A. (1997). Catastro y caracterización de las fuentes de aguas minerales y termales de Chile. Servicio Nacional de Geología y Minería. Boletín N° 50, 89 p. Santiago, Chile. Chile: SERNAGEOMIN, Subdirección Nacional de Geología.
- Hawkins, D. B., & Roy, R. (1963). Experimental hydrothermal studies on rock alteration and clay mineral formation. *Geochimica et Cosmochimica Acta*, 27(10), 1047–1054. [http://doi.org/10.1016/0016-7037\(63\)90065-6](http://doi.org/10.1016/0016-7037(63)90065-6)
- Heimann, A., Beard, B. L., & Johnson, C. M. (2008). The role of volatile exsolution and sub-solidus fluid/rock interactions in producing high ⁵⁶Fe/⁵⁴Fe ratios in siliceous igneous rocks. *Geochimica et Cosmochimica Acta*, 72(17), 4379–4396. <http://doi.org/10.1016/j.gca.2008.06.009>
- Held, S., Schill, E., Sanchez, P., Neumann, T., Emmerich, K., Morata, D., & Kohl, T. (2015). Geological and Tectonic Settings Preventing High-Temperature Geothermal Reservoir Development at Mt . Villarrica (Southern Volcanic Zone): Clay Mineralogy and Sulfate- Isotope Geothermometry. *Proceedings World Geothermal Congress 2015*.
- Hellevang, H., Dypvik, H., Kalleeson, E., Pittarello, L., & Koeberl, C. (2013). Can alteration experiments on impact melts from El'gygytgyn and volcanic glasses shed new light on the formation of the Martian surface? *Meteoritics & Planetary Science*, 48(7), 1287–1295. <http://doi.org/10.1111/maps.12046>
- Kacandes, G. ., & Grandstaff, D. . (1989). Differences between geothermal and experimentally derived fluids: How well do hydrothermal experiments model the composition of geothermal reservoir fluids? *Geochimica et Cosmochimica Acta*, 53(2), 343–358. [http://doi.org/10.1016/0016-7037\(89\)90386-4](http://doi.org/10.1016/0016-7037(89)90386-4)
- Kristmannsdottir, H. (1979). Alteration of Basaltic Rocks by Hydrothermal-Activity at 100-300°C, In: M.M. Mortland and V.C. Farmer, Editor(s). *Developments in Sedimentology, Elsevier*, 27, 359–367.

- Kulik, D. A., Wagner, T., Dmytrieva, S., Kosakowski, G., Hingerl, F. F., Chudnenko, K., & Berner, U. (2013). GEM-Selektor geochemical modeling package: revised algorithm and GEMS3K numerical kernel for coupled simulation codes. *Computational Geosciences*, *17*(1), 1–24. <http://doi.org/10.1007/s10596-012-9310-6>
- Lagat, J. (2010). Hydrothermal alteration mineralogy in geothermal fields with case examples from Olkaria domes geothermal field, Kenya. *Short Course V on Exploration for Geothermal Resources*, 1–24.
- Leturcq, G., Berger, G., Advocat, T., & Vernaz, E. (1999). Initial and long-term dissolution rates of aluminosilicate glasses enriched with Ti, Zr and Nd. *Chemical Geology*, *160*(1-2), 39–62. [http://doi.org/10.1016/S0009-2541\(99\)00055-8](http://doi.org/10.1016/S0009-2541(99)00055-8)
- Liu, L., Suto, Y., Bignall, G., Yamasaki, N., & Hashida, T. (2003). CO₂ injection to granite and sandstone in experimental rock/hot water systems. *Energy Conversion and Management*, *44*(9), 1399–1410. [http://doi.org/10.1016/S0196-8904\(02\)00160-7](http://doi.org/10.1016/S0196-8904(02)00160-7)
- Mayorga, A. Z. (2005). Nicaragua Country Update. *Proceedings World Geothermal Congress 2005*.
- Michard, G. (1991). The physical chemistry of geothermal systems. In *Applications of Geochemistry in Geothermal Reservoir Development* (pp. 197–214).
- Moreno, H., & Lara, L. (2008). Geología del Área Pucón-Curarrhue, Regiones de La Araucanía y de Los Ríos, Servicio Nacional de Geología y Minería. Carta Geológica de Chile. Serie Geología Básica 115: 36p., 1 mapa escala 1:100.000. Santiago.
- Parkhurst, D. L., & Appelo, C. A. J. (2013). Description of input and examples for PHREEQC version 3--A computer program for speciation, batch- reaction, one-dimensional transport, and inverse geochemical calculations: U.S. Geological Survey Techniques and Methods, book 6, chap. A43, 497 p., availab.
- Paul, A. (1977). Chemical durability of glasses; a thermodynamic approach. *Journal of Materials Science*, *12*(11), 2246–2268. <http://doi.org/10.1007/BF00552247>
- Pérez, Y. (1999). Fuentes de aguas termales de la cordillera andina del centro-sur de Chile (39–42°S). Servicio Nacional de Geología y Minería. Boletín No. 54, 65p.. 12 anexos, 1 mapa 1:500.000. Santiago. SERNAGEOMIN, Subdirección Nacional de Geología.
- Pérez-Zárate, D., Torres-Alvarado, I. S., Santoyo, E., & Díaz-González, L. (2010). Analysis of Experimental Variables during Water-Rock Interaction Experiments for Solute Geothermometer Calibration. *Proceedings World Geothermal Congress 2010*, (April), 25–29.
- Petersen, S., & Hack, K. (2007). The thermochemistry library ChemApp and its applications. *International Journal of Materials Research*, *98*(10), 935–945. <http://doi.org/10.3139/146.101551>
- Pirajno, F. (2009). Hydrothermal Processes and Wall Rock Alteration. In *Hydrothermal Processes and Mineral Systems* (pp. 73–164).
- Potter, J., Dibble, W., Parks, G., & Nur, A. (1982). *Improvements in geothermometry*. (T. ~W. Simon, R. ~J. Moffat, J. ~P. Johnston, & W. ~M. Kays, Eds.) *Stanford Univ. Report*.
- Powell, T., & Cumming, W. (2010). SPREADSHEETS FOR GEOTHERMAL WATER AND GAS GEOCHEMISTRY. *Proceedings. Thirty-Fifth Workshop on Geothermal Engineering*.
- Protti, A. M. (2010). Costa Rica Country Update Report. *Proceedings World Geothermal Congress 2010*.
- Reyes, A. G. (1990). Petrology of Philippine geothermal systems and the application of alteration mineralogy to their assessment. *Journal of Volcanology and Geothermal Research*, *43*, 279–309.
- Risacher, F., Fritz, B., & Hauser, A. (2011). Origin of components in Chilean thermal waters. *Journal of South*

American Earth Sciences, 31(1), 153–170. <http://doi.org/10.1016/j.jsames.2010.07.002>

- Risacher, F., & Hauser Y., A. (2008). Catastro de las principales fuentes de aguas termales de Chile. Informe Ird / Sernageomin, Santiago, Chile.
- Robert, C., & Goffé, B. (1993). Zeolitization of basalts in subaqueous freshwater settings: Field observations and experimental study. *Geochimica et Cosmochimica Acta*, 57(15), 3597–3612. [http://doi.org/10.1016/0016-7037\(93\)90142-J](http://doi.org/10.1016/0016-7037(93)90142-J)
- Rodríguez, A. (2011). *Water-rock interaction of silicic rocks: an experimental and geochemical modelling study*. University of Iceland.
- Rodríguez, J. A., & Herrera, A. (2005). El Salvador Country Update. *Proceedings World Geothermal Congress 2005*.
- Sánchez, P., Pérez-Flores, P., Arancibia, G., Cembrano, J., & Reich, M. (2013). Crustal deformation effects on the chemical evolution of geothermal systems: the intra-arc Liquiñe–Ofqui fault system, Southern Andes. *International Geology Review*, 55(11), 1384–1400. <http://doi.org/10.1080/00206814.2013.775731>
- Savage, D. (1986). Granite-water interactions at 100°C, 50 MPa: An experimental study. *Chemical Geology*, 54(1-2), 81–95. [http://doi.org/10.1016/0009-2541\(86\)90073-2](http://doi.org/10.1016/0009-2541(86)90073-2)
- Savage, D., Bateman, K., & Richards, H. G. (1992). Granite-water interactions in a flow-through experimental system with applications to the Hot Dry Rock geothermal system at Rosemanowes, Cornwall, U.K. *Applied Geochemistry*, 7(3), 223–241. [http://doi.org/10.1016/0883-2927\(92\)90039-6](http://doi.org/10.1016/0883-2927(92)90039-6)
- Savage, D., & Chapman, N. A. (1982). Hydrothermal behaviour of simulated waste glass—And waste—Rock interactions under repository conditions. *Chemical Geology*, 36(1-2), 59–86. [http://doi.org/10.1016/0009-2541\(82\)90039-0](http://doi.org/10.1016/0009-2541(82)90039-0)
- Sernageomin. (2003). Mapa geologico de chile: version digital. *Publicacion Geologia Digital*, 4, 25. Retrieved from <http://geoportal.sernageomin.cl/geovisor/GeoVisor/index.html?resources=map:ags@http://geoarcgis.sernageomin.cl/ArcGIS/rest/services/geoportal/GeologiaBase/MapServer>
- Seyfried, W. E., & Bischoff, J. L. (1979). Low temperature basalt alteration by sea water: an experimental study at 70°C and 150°C. *Geochimica et Cosmochimica Acta*, 43(12), 1937–1947. [http://doi.org/10.1016/0016-7037\(79\)90006-1](http://doi.org/10.1016/0016-7037(79)90006-1)
- Shiraki, R., & Iiyama, J. T. (1990). Na-K ion exchange reaction between rhyolitic glass and (Na, K)Cl aqueous solution under hydrothermal conditions. *Geochimica et Cosmochimica Acta*, 54(11), 2923–2931. [http://doi.org/10.1016/0016-7037\(90\)90110-7](http://doi.org/10.1016/0016-7037(90)90110-7)
- Stoffregen, R. E., & Cygan, G. L. (1990). An experimental study of Na-K exchange between alunite and aqueous sulfate solutions. *American Mineralogist*, 75, 209–220.
- Tardani, D., Reich, M., Roulleau, E., Takahata, N., Sano, Y., González-Jiménez, J. M., ... Arancibia, G. (2015). Metal Fluxing in a Large-Scale Intra-Arc Fault : Insights from the Liquiñe-Ofqui Fault System in Southern Chile. In *Congreso Geologico Chileno* (pp. 2–5).
- Techer, I., Advocat, T., Lancelot, J., & Liotard, J.-M. (2001). Dissolution kinetics of basaltic glasses: control by solution chemistry and protective effect of the alteration film. *Chemical Geology*, 176(1-4), 235–263. [http://doi.org/10.1016/S0009-2541\(00\)00400-9](http://doi.org/10.1016/S0009-2541(00)00400-9)
- Wagner, T., Kulik, D. A., Hingerl, F. F., & Dmytrievava, S. V. (2012). Gem-selector geochemical modeling package: TSolMod library and data interface for multicomponent phase models. *Canadian Mineralogist*, 50(5), 1173–1195. <http://doi.org/10.3749/canmin.50.5.1173>

Wolery, T. J. (1992). EQ3/6, A software package for geochemical aqueous systems: Package Overview and installation guide (Ver.7.0).

11 Appendix

11.1 Outcrop and hand sample descriptions

11.1.1 Sample IV-1

Fine grain gray sandstones with varves intercalated with mid grain sandstones with ondulites. 5 samples, no weathering, S/D=N90°E/45



11.1.2 Sample IV-4

Pyroclastic deposit, lapilli tuff (or volcanic breccia?), with a 60% matrix composed of mid grain ash (55%) and plagioclase (5%, 2 mm long) and the pyroclasts composed mostly of lavas. 2 samples, very hard rock, no weathering. Large outcrop (100m)



11.1.3 Sample IV-5

Pyroclastic flux deposit, with coarse grain ash matrix (65%) and polymictic volcanic and intrusive clasts from 5 mm to 1 m. 3 samples, large outcrop (20 m), no weathering, thermal waters up flow on winter according to owner.



11.1.4 Sample IV-6

Andesitic-dacitic lava, with 45% groundmass, 30% plagioclase and 25% quartz. 2 samples, good outcrop. 10 m.



11.1.5 Sample IV-7

Pyroclastic breccia. Green and purple matrix (25%) composed of mid grain ash, clasts are polymictic, volcanic and angular. 2 samples, good outcrop. 2 m high. Important hydrothermal alteration: red veins of 5-10 cm thick, and chloritization of matrix, near Los Pozones



11.1.6 Sample IV-8

Oligomictic conglomerate composed mainly by rounded clasts of andesitic lava, 75% groundmass, 10% mafic minerals (1 mm), 15% plagioclase (<1 mm). Very good outcrop (>80 m rock wall), no weathering, cold waters spring out from the fractures of the rock wall (fractures are $\sim 5/m^2$)



11.1.7 Sample IV-9

Andesitic porfídic lava, 95% groundmass, 5% plagioclase (1-3 mm). Good outcrop, near Colico lake.



11.1.8 Sample IV-10

Lava with 2 -20 mm long horizontal amygdalae (5%), a 5% of 1 cm long plagioclases on a vitreous groundmass. Good outcrop, it seems that the outcrop represents the trace of an important subvertical N30°O structure.



11.1.9 Sample IV-11

Stratified deposits of some kind. Possibly very fine grain ash in a fall deposit. Intercalated with polymictic lapilli tuff. Good outcrop, also with major structures that break the formation and mix the 2 lithologies.

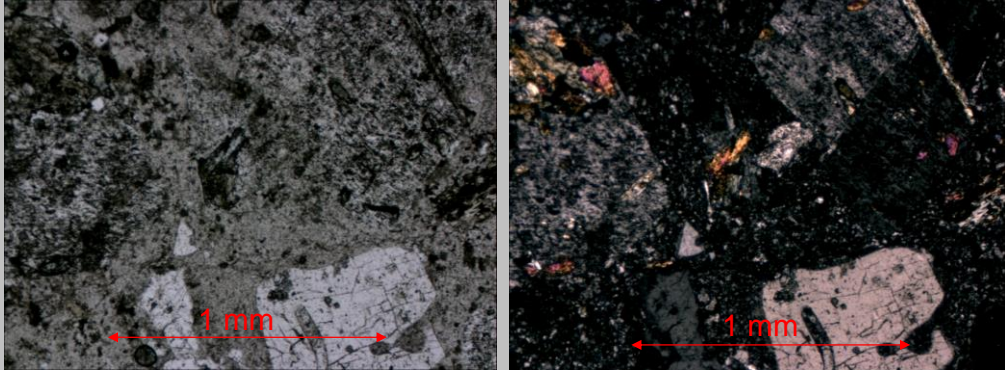
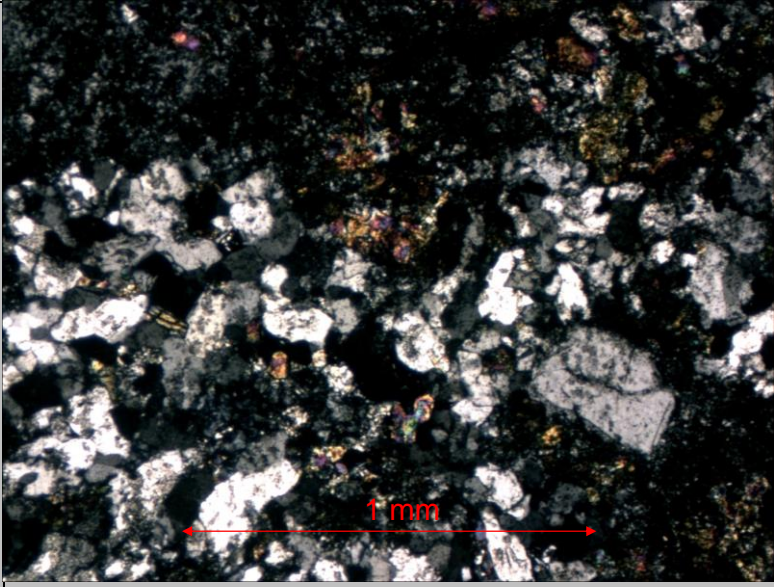


11.2 Thin sections descriptions

Rock sample: IV - 1				
Primary minerals				
Matrix minerals (100%)	Abundance (%)	Size (longitude)	Shape	Obs
Quartz	15%	0.01 - 0.08 mm	angular	quartz shows low reworking evidences
K-Feld	10%	0.01 - 0.08 mm	angular	
Plagioclase	25%	0.01 - 0.08 mm	angular	
Opagues	15%	0.005 to 0.1 mm	poorly rounded, better	possibly hematite or some kind of FeOx, some red color is observed
hornblende	5%	0.03 mm	poorly rounded, better than quartz	
other magmatic mafics	2%	0.03 mm	poorly rounded, better than quartz	
undifferentiated small size family of grains, possibly same minerals	28%			
Photomicrographys				
Description	Parallel (left) and Crossed (right) Polars Photomicrographys of IV-1			

Rock sample: IV - 4 Porphyric andesite with clinopyroxene				
<i>Primary minerals</i>				
Phenocrysts (35%)	Abundance (%)	Size (longitude)	Shape	Obs
Plagioclase	25	0.2 - 2.5 mm	subhedral, tabular	Can also be found in the lithics as phenocryst in a groundmass of FeOX
Clinopyroxene	10	0.2 - 0.8 mm	subhedral, prismatic	also found as clusters of phenocrysts
Groundmass (65%)	Plagioclase, pyroxene and magnetite minerals (0,01 mm)			
<i>Alteration minerals</i>				
Mineral	Abundance (%)	Size	Shape	Obs
Chlorite	6	0.02 mm	radial, acicular	filling spaces
Chalcedony	4		radial, acicular	filling spaces
Clay	5			replacing the plagioclase
<i>Photomicrographs</i>				
Description	Crossed Polars Photomicrographs of IV-4, showing on the left, clinopyroxene and plagioclase phenocrysts and on the right, cavities filled by chlorite and chalcedony.			

Rock sample: IV - 5				
<i>Primary minerals</i>				
Pyroclastic fragments (40%)	Abundance (%)	size	mineral	mineral abundance (%)
Lithics	35	more than 1 m (outcrop)	Plagioclase	50
			Olivine	7
			Pyroxene (ortho and clin)	8
			glass (in lithics as groundmass)	35
Single Crystals	5	0.5 - 1 mm	same minerals as clasts	
Matrix (60%)				
crystals	30	0.01 - 0.05 mm	Mostly plagioclase, same proportion as in lithics	
lithics	5	0.01-0.03 mm		
glass (volcanic ash)	25			
<i>Alteration minerals</i>				
Mineral	Abundance (%)	Size	Shape	Obs
iddignsite	2			replacing olivine
Clorite	3			
Unknown	10			opaque mineral replacing glass in lithic's groundmass
<i>Photomicrographs</i>				
Description	Crossed (left) and Parallel (right) Polars Photomicrographs of IV-5, showing the andesitic lithic clasts and plagioclase, olivine and pyroxene minerals in an ash matrix.			
General observations	The rock represents a pyroclastic deposit of some sort, probably a density current or a lahar deposit. All lithics are volcanic and the matrix presents vitreous ash and lithics of the same type. The lithics are all andesitic with the same mineralogy but different primary textures and mineral sizes, no quartz is identified at thin cut although it might have a little.			

Rock sample: IV - 6: dacite lava with biotite				
Primary minerals				
Phenocrysts (45%)	Abundance (%)	Size (longitude)	Shape	Obs
Quartz	15	0.1 - 1 mm	subhedral	presents notorious absorption textures, single phenocrysts
plagioclase	30	0.1 - 2 mm	subhedral, tabular	also presents absorption textures (sieves)
biotite	<1	0.3 mm	tabular	probably the most affected mineral by alteration, chloritized
Groundmass (55%)	Mostly glass and opaques (magnetite, titanite.. etc) presents important alteration to chlorite and clays			
Alteration minerals				
Mineral	Abundance (%)	Size	Shape	Obs
quartz	5	0.1 mm	anhedral	it's concentrated mostly on a quartz-epidote 2 mm thick vein
clay	20			mostly on plagioclase and groundmass
Chlorite	10	<0.01 mm	anhedral	Altering all minerals except quartz, also in groundmass
epidote	10	0.05 - 0.3 mm	subhedral	concentrated on a quartz-epidote 2 mm thick vein but disseminated also
actinolite	2	0.1 - 1 mm	subhedral	disseminated
Photomicrographs				
				
Description	<p>Parallel (left) and Crossed (right) Polars Photomicrographs of IV-6, showing altered groundmass (mostly chlorite and clay), a plagioclase (left center and top right) and a quartz (bottom right) phenocrysts with absorption textures, a deeply altered biotite (right centre), epidote and actinolite with third and second order interference colors (mostly on plagioclases)</p>			
Second photomicrography showing the quartz and actinolite alteration minerals.				

Rock sample: IV - 7 sedimentary conglomerate with volcanic clasts

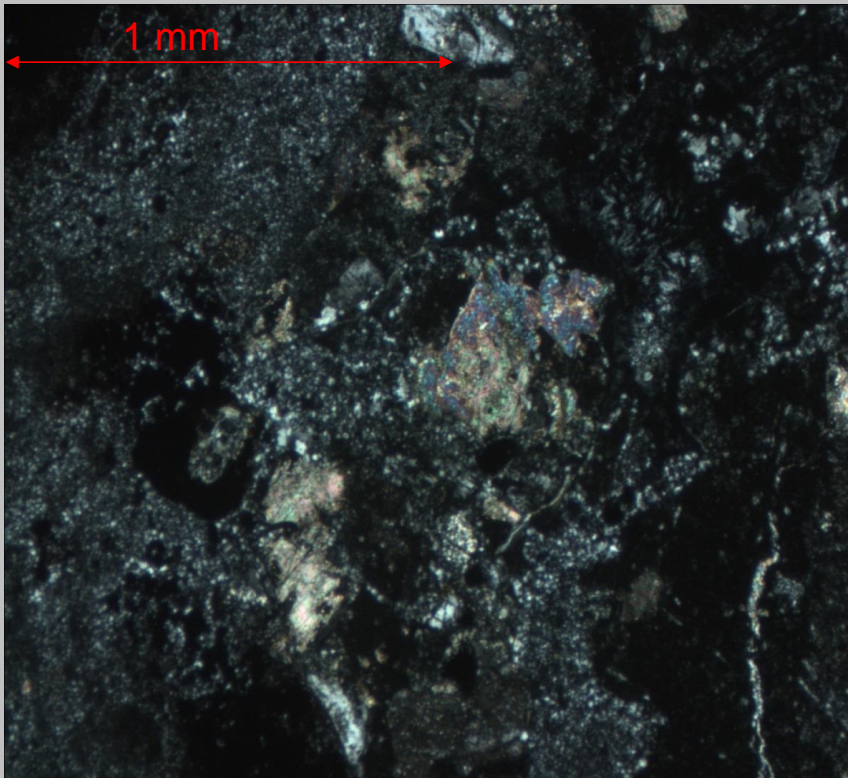
Primary minerals

Phenocrysts (%)	Abundance (%)	Size (longitude)	Shape	Obs
Plagioclase	15	0.1 - 1 mm	subhedral, tabular	highly altered to calcite and Qtz
Groundmass (%)	Presumable glass, highly altered			

Alteration minerals

Mineral	Abundance (%)	Size	Shape	Obs
Quartz	60%	<0.01 to 0.1 mm	granular, anhedral	hydrothermal quartz as veins and replacing groundmass in clasts groundmass
Calcite	20%	<0.01 mm at clasts groundmass, 0.1-0.5 mm on plagioclase	anhedral, shapeless	all over the rock
Opaque	3%	0.1 - 0.3 mm	cubic	No metallic luster is observed at hand sample, probably magnetite
hematite	5%	cryptocrystalline		filling spaces around clasts
zeolite	2%	0.05 mm	anhedral, granular	filling small spaces inside clasts

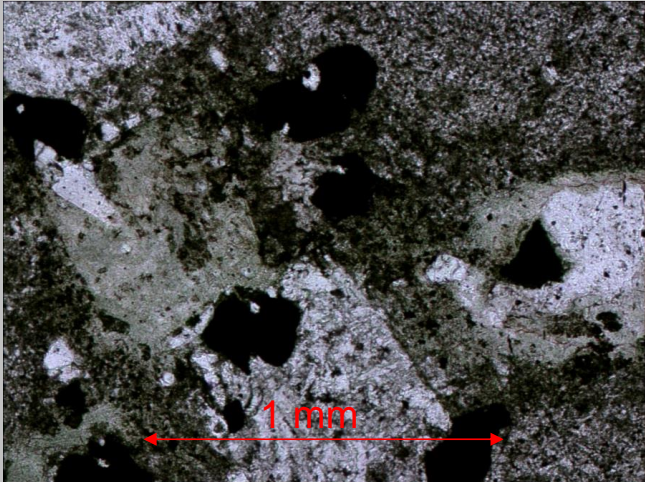
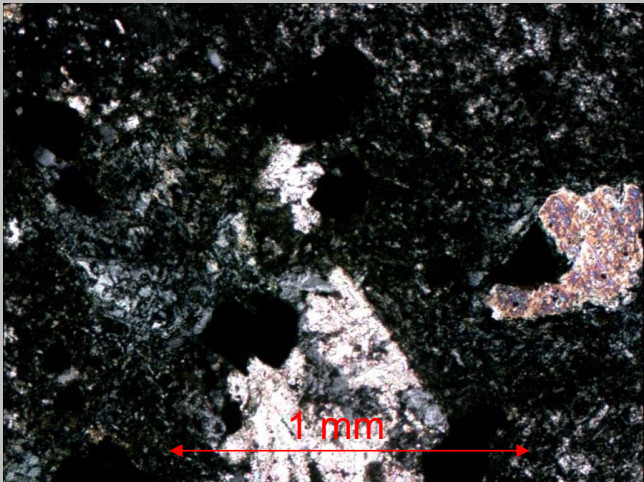
Photomicrographs



Description	at the photomicrography it is possible to see the deep calcite and quartz alteration and a zeolite domain at the center-right portion.
-------------	--

General observations	Rock is clastic with volcanic clasts, in thin cut only porphyritic lavas with plagioclase phenocrysts are observed, but at outcrop some intrusive clasts were seen also.
----------------------	--

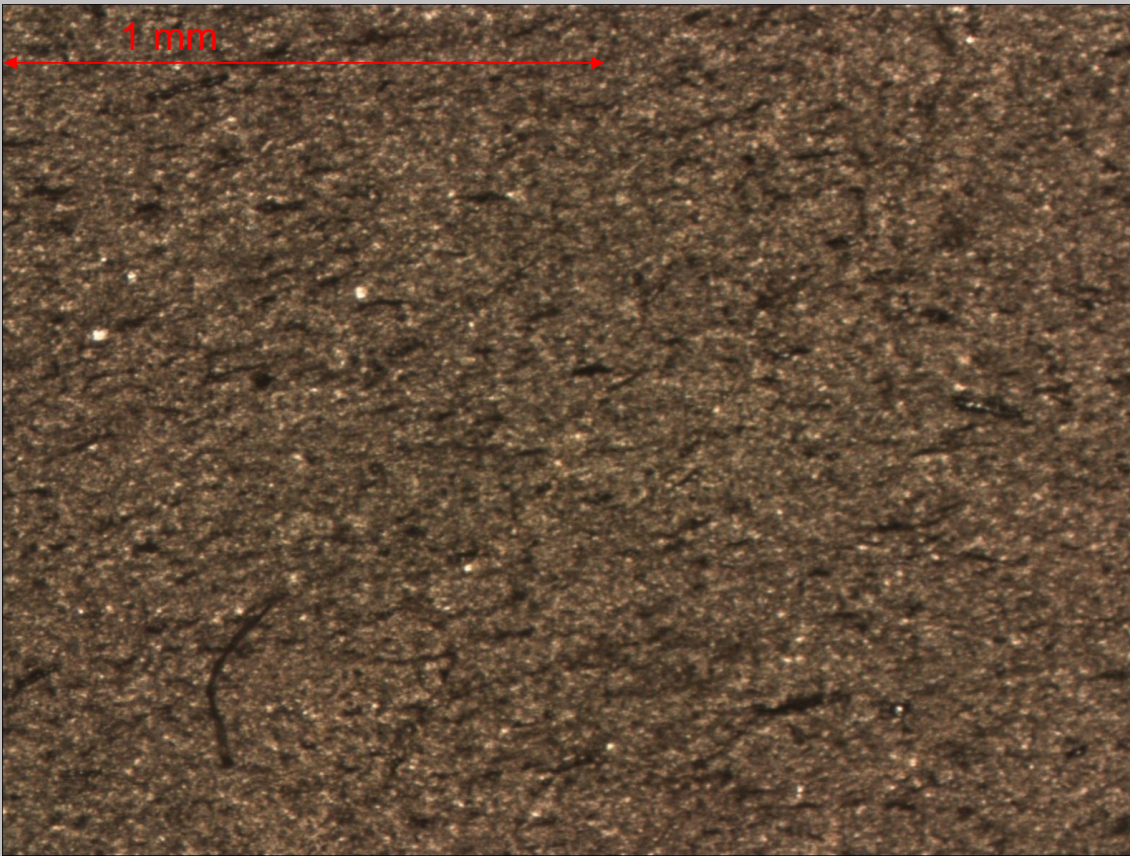
Rock sample: IV - 8 Thick Conglomerate (sedimentary, volcanic material)				
Primary minerals				
Clasts Phenocrysts (2%)	Abundance (%)	Size (longitude)	Shape	Obs
Pyroxene	1	0.1 mm	euhedral, prismatic	completely replaced by secondary minerals (pseudomorph)
Muscovite	1	0.2 mm	anhedral, tabular	
Clasts Groundmass (58%)	Composed by elongated 0.03-0.1 mm plagioclase, magnetite and pyroxene.			
Matrix (40%)	0.01 mm to 1 mm lava fragments composed mostly by plagioclase (50% of matrix clasts) but also pyroxene, magnetite, quartz and hornblende			
Alteration minerals				
Mineral	Abundance (%)	Size	Shape	Obs
Chlorite	10			mostly on matrix
Calcite	15			Mostly on clasts
Photomicrographs				
Description	Crossed (left) and Parallel (right) Polars Photomicrographs of IV-8, showing the calcite alteration on the left and the chloritization of the matrix on the right.			
General Observations				
Although the hand sample looks like lava, the flat surface left by the saw made a clear face to see the rounded volcanic monomictic clasts.				

Rock sample: IV - 9: Andesite lava with clinopyroxene				
<i>Primary minerals</i>				
Phenocrysts (20%)	Abundance (%)	Size (longitude)	Shape	Obs
Plagioclase	10	0.5 - 5 mm	subhedral, tabular	
Clinopyroxene	5	0.2 - 1 mm	euohedral, prismatic	most of the crystals are completely altered, except for a few specific
Magnetite	5	0.1 - 0.3 mm	euohedral, cubic	
Groundmass (80%)	Deeply altered, composed of plagioclase (20%, <0.05mm) and magnetite (euohedral). It possibly had glass and/or pyroxene but the alteration left only the other two recognizable			
<i>Alteration minerals</i>				
Mineral	Abundance (%)	Size	Shape	Obs
Chlorite	5	<0.05 mm	anhedral	Altering most of the pyroxenes (95%)
Clay	18	cryptocrystalline	anhedral	Partially in the plagioclase (10%), mostly in the groundmass (20%)
Calcite	5	0.05 - 0.2 mm	anhedral	Altering partially the plagioclase (50%)
<i>Photomicrographs</i>				
				
Description	<p>Parallel (left) and Crossed Polars Photomicrographs of IV-9, show the altered groundmass, the plagioclase (left top and bottom centre) altered to carbonated minerals (bottom centre). Also the pyroxenes deeply altered to chlorite except for the one in the right (left centre and right centre).</p>			

Rock sample: IV - 10 porphyric dacite				
<i>Primary minerals</i>				
Phenocrysts (10%)	Abundance (%)	Size (longitude)	Shape	Obs
plagioclase	2	0.3 mm	subhedral, tabular	
Sanidine (K-feld)	8	0.5 - 3 mm	subhedral, tabular	
Groundmass (90%)	composed mostly by elonged 0.1mm plagioclase and feldespar, might have quartz but its hard to tell. Also opaques (Magnetite?)			
<i>Alteration minerlas</i>				
Mineral	Abundance (%)	Size	Shape	Obs
Chlorite	15%	<0.1		mostly on groundmass
Clay	5			on feldespars and groundmass
quartz	3	0.2 0.5 mm	anhedral	filling eliptical orientated cavities with quartz and calcite.
calcite	10	0.1 - 2 mm	anhedral	filling eliptical orientated cavities with quartz and calcite. (>Calcite than Qtz)
<i>Photomicrographys</i>				
Description	On the left, a sanidine crystal. On the right one of the elonged cavities filled with Qtz and calcite			

Rock sample: IV - 11

Photomicrographs

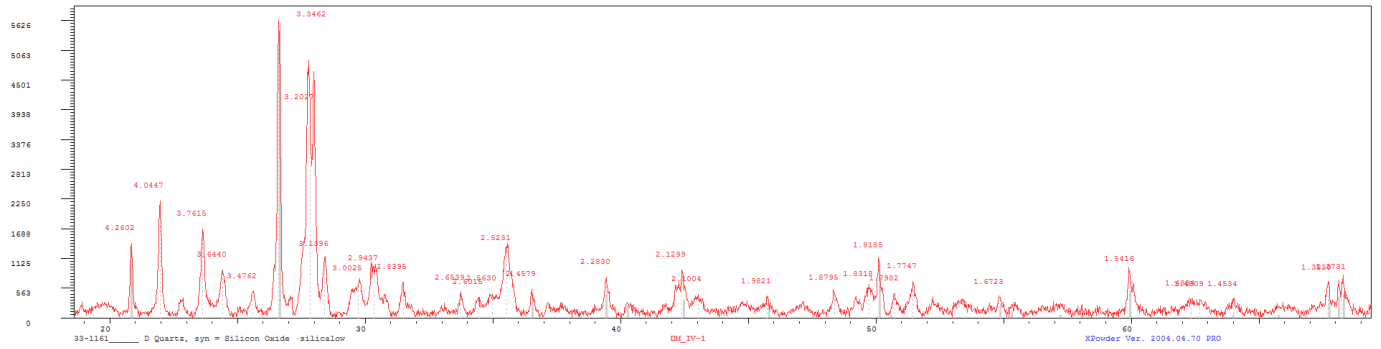


Description

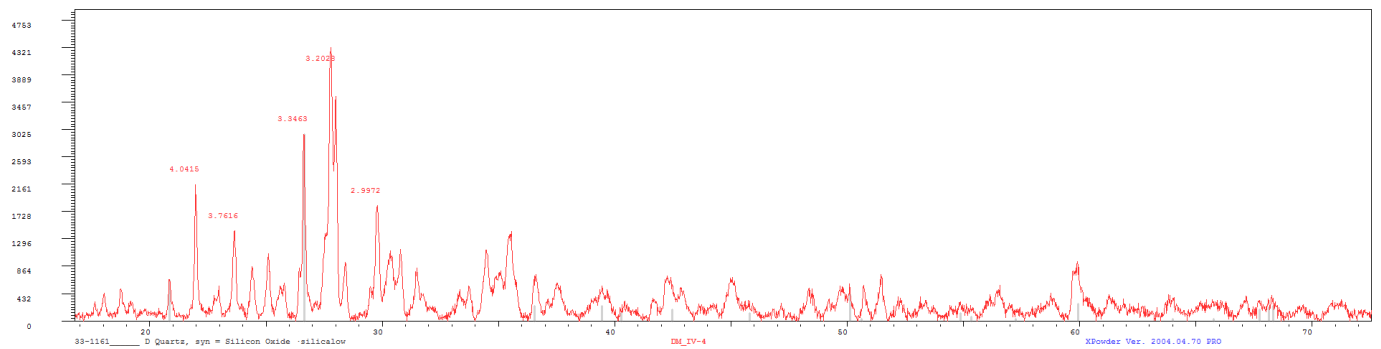
although some thin bedding structures are visible, grainsize is too small to be able to recognize specific minerals.

11.3 Results of XRD analysis

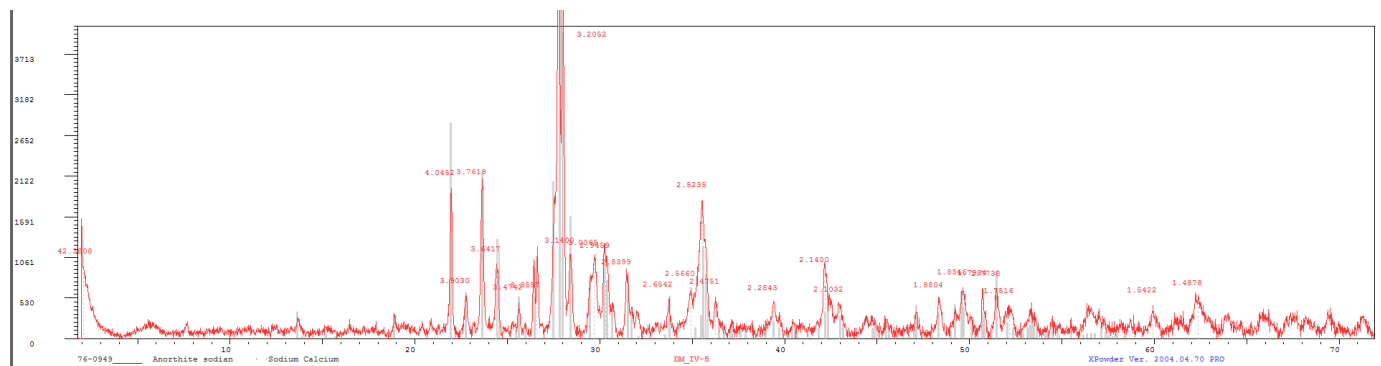
IV-1



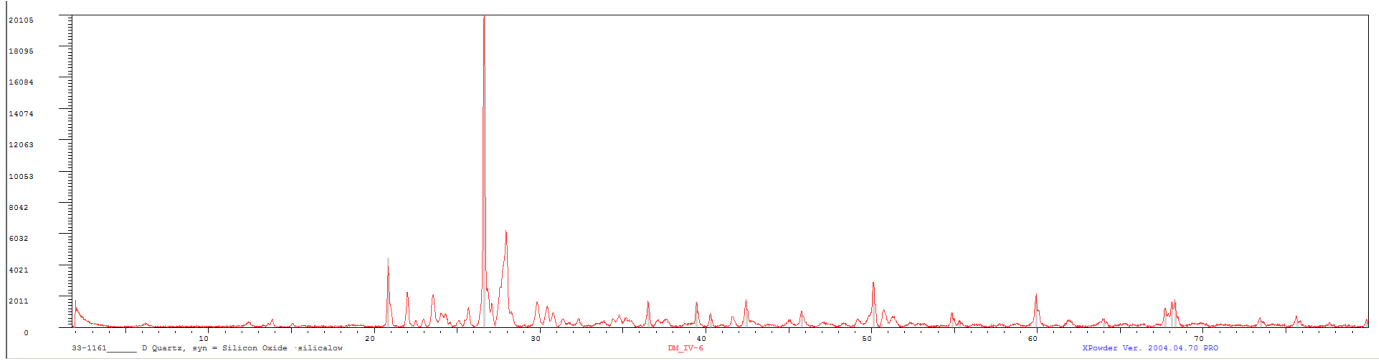
IV-4



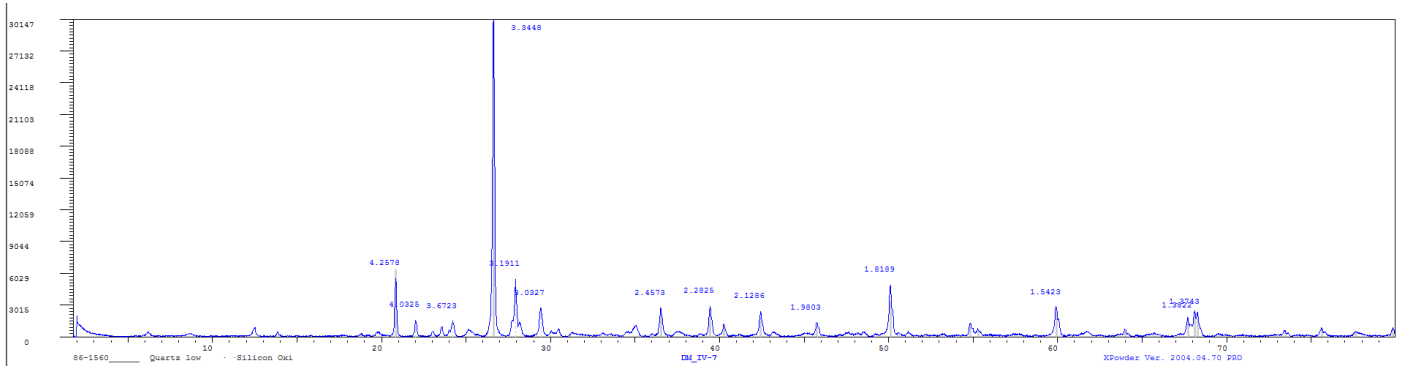
IV5



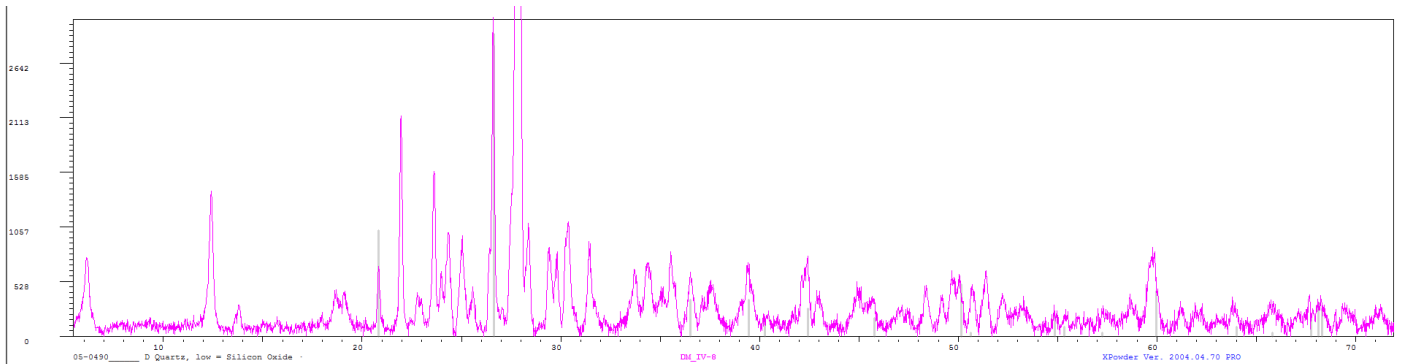
IV-6



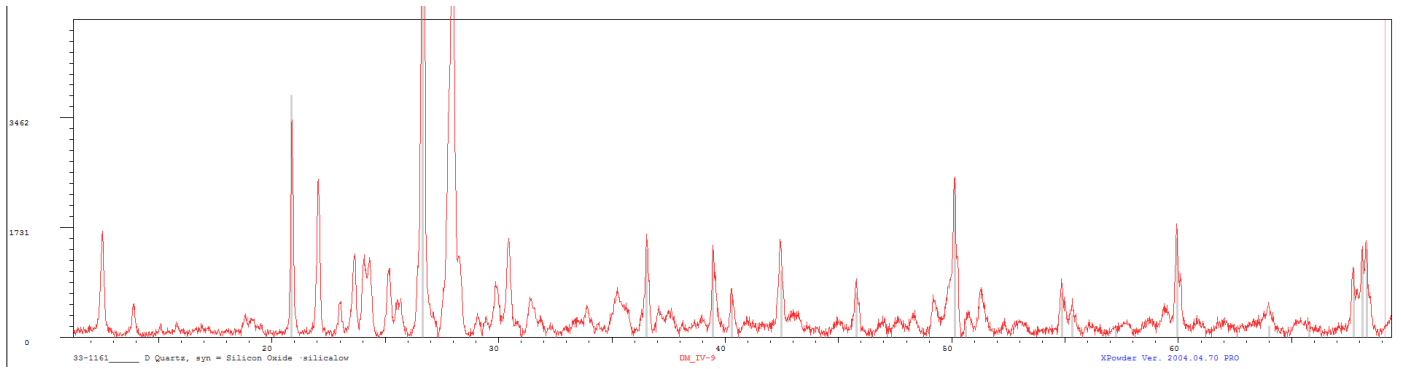
IV-7



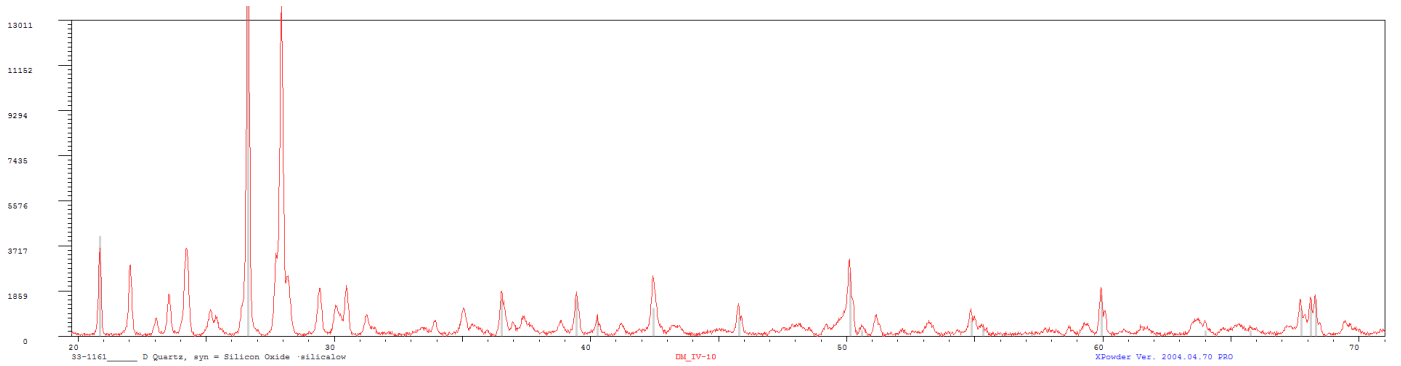
IV-8



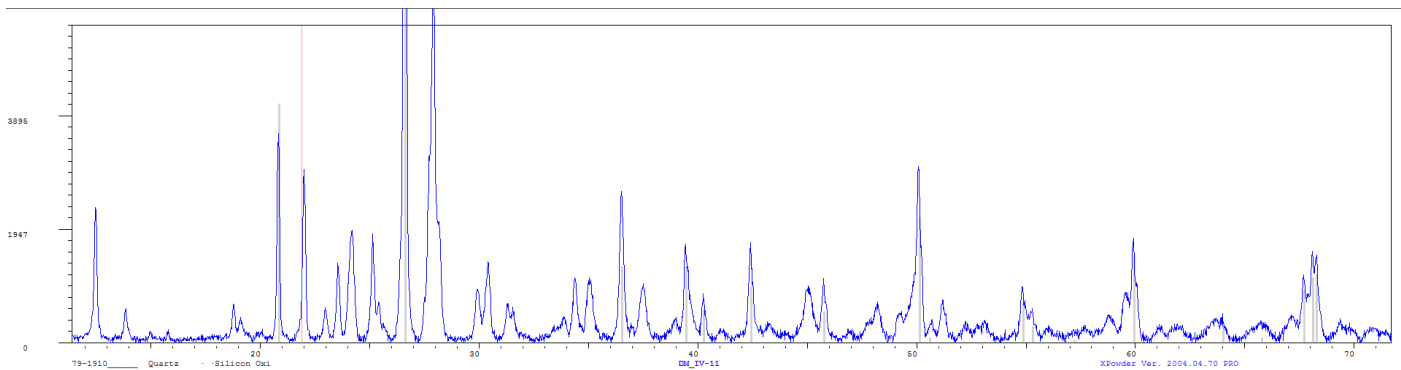
IV-9



IV-10



IV-11



11.4 Matlab code used to obtain logK for glass

```

clc
clear

T=[0 25 60 100 150 200 250 300];
%Logk for 0 25 60 100 150 200 250 300°C
logk=[
-2.947 -2.714 -2.445 -2.202 -1.971 -1.802 -1.684 -1.605; %SiO2
-63.369 -60.908 -58.656 -56.998 -55.809 -55.425 -55.928 -57.757; %AlO1.5
15.228 13.532 11.58 9.799 8.039 6.626 5.437 4.381; %FeO
23.742 21.335 18.58 16.082 13.638 11.702 10.101 8.716; %MgO
35.681 32.576 29.011 25.7564 22.545 19.988 17.875 16.058; %CaO
73.075 67.427 60.985 55.166 49.514 45.114 41.587 38.675; %(NaO0.5)
9.879 84.041 76.192 69.037 62.01 56.474 51.993 48.275]; % (KO0.5)

% mol=[1 0.321 0.091 0.151 0.122 0.119 0.017]; %Si Al Fe Mg Ca Na K ///do not
use more than 3 decimal numbers
%mol=[1 0.342 0.037 0.018 0.158 0.037 0.018]; %IV-5
%mol=[1 0.069 0.001 0.001 0.027 0.051 0.138]; %IV-6
mol=[1 0.415 0.213 0.075 0.385 0.085 0.034]; %IV-5
molf=mol/sum(mol); %Si Al Fe Mg Ca Na K
glass=zeros(1,length(T)); %mol fraction

for i=1:length(T)
    glass(i)=sum(logk(:,i).*molf') + sum(molf.*log10(molf));
end

O=sum([2 1.5 1 1 1 .5 .5].*mol); %total oxigen mols in oxides
H2O=sum([0 2.5 -1 -1 -1 -.5 -.5].*mol); %total water mols (reactant)
H=sum([0 -1 2 2 2 1 1].*mol); %total H+ mols reactant

%log10K=a1 + a2*x + a3/x + a4*log10(x) + a5/x^2 + a6*T^2

%since you cant devide by 0,

T(1)=2;

%formula:
formula=['SiAl' num2str(mol(2)) 'Fe' num2str(mol(3)) 'Mg' num2str(mol(4)) 'Ca'
num2str(mol(5)) 'Na' num2str(mol(6)) 'K' num2str(mol(7)) 'O' num2str(O) ' + ' num2str(H) 'H+
+ ' num2str(H2O) 'H2O = SiO2 + ' num2str(mol(2)) 'Al(OH)4- + ' num2str(mol(3)) 'Fe+2 + '
num2str(mol(4)) 'Mg+2 + ' num2str(mol(5)) 'Ca+2 + ' num2str(mol(6)) 'Na+ + ' num2str(mol(7))
'K+' ];
disp(formula)
%for opening curve fit tool write "cftool" command
%use T as x and glass as y
%use custom equation a1 + a2*x + a3/x + a4*log10(x) + a5/x^2 + a6*T^2

%example Phreeqc entry:
%PHASES
%basaltic_glass
% SiAl0.36Fe0.19Mg0.28Ca0.26Na0.08K0.008O3.314 + 1.188H+ + 0.126H2O = SiO2 + 0.36Al(OH)4-
+ 0.19Fe+2 + 0.28Mg+2 + 0.26Ca+2 + 0.08Na+ + 0.008K+
% -analytical_expression -0.0003083 -1.768 12.34 0.2072 0.9977 0.7835

```


11.5 Phreeqc Models input

11.5.1 IV-4

```
#FinalFinal
SOLUTION 1
  temp      140
  pe        -4
  redox     pe
  units     mg/kgw
  density   1
  #villarrica lake water composition (risacher 2011)
  pH        7.06
  Ca        4.8
  Cl        1.3
  K         0.9
  Mg        1.75
  Na        3.9
  Si        10.7
  S(6)      1.4
  C(4)      30.7
  -water    1 # kg
EQUILIBRIUM_PHASES 1
  Albite    0 0.279664454
  Anorthite 0 0.215669077 dissolve_only
  Chalcedony 0 0.554788099
  Clinocllore-14A 0 0.028787852 dissolve_only
  Diopside  0 0.230896757 dissolve_only
  Hedenbergite 0 0.053744587 dissolve_only
  K-Feldspar 0 0.110182148
  Kaolinite 0 0.129120393
  Magnetite 0 0.100778441 dissolve_only
  Mordenite 0 0
  Nontronite-Ca 0 0
  Nontronite-Mg 0 0
```

11.5.2 IV-5

```
#SOLUTION 1
  temp      140
  pe        -4
  redox     pe
  units     mg/kgw
  density   1
  #villarrica lake water composition (risacher 2011)
  pH        7.06
  Ca        4.8
  Cl        1.3
  K         0.9
  Mg        1.75
  Na        3.9
  Si        10.7
  S(6)      1.4
  C(4)      30.7
```

```

-water      1 # kg
EQUILIBRIUM_PHASES 1
Albite 0 0.266952433
K-Feldspar 0 0.059881602
Anorthite 0 0.275577154 dissolve_only
Quartz 0 0.665745718
Diopside 0 0.100055261 dissolve_only
Forsterite 0 0.123201437 dissolve_only
Ferrosilite 0 0.079103792 dissolve_only
Hematite 0 0.020874168 dissolve_only
andesite_glass 0 0.531003046
Nontronite-Ca 0 0
Saponite-Ca 0 0
Prehnite 0 0
Mesolite 0 0
Greenalite 0 0

SOLUTION_SPECIES
#Al(OH)4-      82
Al+3 + 4H2O = Al(OH)4- + 4H+
log_k          -22.7
delta_h 42.3 kcal
-analytical    51.578          0.0      -11168.9      -14.865          0.0
-gamma 4.5      0.0

PHASES
#SEM-EDS RESULTS
andesite_glass
SiAl0.415Fe0.213Mg0.075Ca0.385Na0.085K0.034O3.355 + 1.05H+ + 0.305H2O = SiO2 +
0.415Al(OH)4- + 0.213Fe+2 + 0.075Mg+2 + 0.385Ca+2 + 0.085Na+ + 0.034K+
-analytical_expression -2.527 -0.01492 -2.913 -0.6156 -1.462 2.092

```

11.5.3 IV-6

```

SOLUTION 1
temp      140
pe        -4
redox     pe
units     mg/kgw
density   1
pH        7.06
Ca        4.8
Cl        1.3
K         0.9
Mg        1.75
Na        3.9
Si        10.7
S(6)     1.4
C(4)     30.7
-water    1 # kg
EQUILIBRIUM_PHASES 1
Albite 0 0.063560103
K-Feldspar 0 0.28743169
Anorthite 0 0.035944846 dissolve_only
Magnetite 0 0.01439692 dissolve_only
Kaolinite 0 0.025824079
Quartz 0 2.163673585

```

```

Epidote 0 0.027592962 dissolve_only
Clinochlore-14A 0 0.011994938
andesite_glass 0 0.693058783 dissolve_only
Mordenite 0 0
Montmor-Ca 0 0
Nontronite-Ca 0 0
Saponite-Ca 0 0
SOLUTION_SPECIES
#Al(OH)4- 82
  Al+3 + 4H2O = Al(OH)4- + 4H+
  log_k -22.7
  delta_h 42.3 kcal
  -analytical 51.578 0.0 -11168.9 -14.865 0.0
  -gamma 4.5 0.0
PHASES
#SEM-EDS RESULTS
andesite_glass
  SiAl0.39Fe0.04Mg0.018Ca0.0389Na0.331K0.004O2.8494 + 0.1388H+ + 0.7106H2O = SiO2 +
0.39Al(OH)4- + 0.04Fe+2 + 0.018Mg+2 + 0.0389Ca+2 + 0.331Na+ + 0.004K+
  -analytical_expression -2.029 -0.01683 12.5 0.4022 -21.52 0.6081

```

11.5.4 IV-8

```

SOLUTION 1
  temp 140
  pe -4
  redox pe
  units mg/kgw
  density 1
  pH 7.06
  Ca 4.8
  Cl 1.3
  K 0.9
  Mg 1.75
  Na 3.9
  Si 10.7
  S(6) 1.4
  C(4) 30.7
  -water 1 # kg
EQUILIBRIUM_PHASES 1
  Albite 0 0.457632742
  Anorthite 0 0.173733423 dissolve_only
  K-Feldspar 0 0.00598816
  Chamosite-7A 0 0.046718711
  Clinochlore-14A 0 0.047979753
  Magnetite 0 0.01439692 dissolve_only
  Quartz 0 0.554788099
  Diopside 0 0.015393117 dissolve_only
  Hedenbergite 0 0.04030844 dissolve_only
  Forsterite 0 0.071077752 dissolve_only
  Ferrosilite 0 0.065432929 dissolve_only
  Calcite 0 0.099914074
  Muscovite 0 0.050213029 dissolve_only
  Saponite-Ca 0 0
  Nontronite-Na 0 0
  Montmor-Mg 0 0

```

11.6 Detailed water composition of alteration experiments: blind and exp(IV-4).

Days	Li	B	Na	Mg	Al	P	K	Ca
	[µg/L]	[µg/L]	[mg/L]	[mg/L]	[µg/L]	[µg/L]	[mg/L]	[mg/L]
10	6.13	50.8	79.4	0.11	480.2	<2,4	51.5	11.9
20	7.2	50.9	87.3	0.08	348.8	<2,4	18.8	11.2
30	7.18	51.3	90.7	0.06	472.4	<2,4	13.8	9.35
45	9.332	56.34	96.58	0.147	225.39	<2,5	16.174	16.71
60	10.462	56.68	99.06	0.153	366	10.108	74.86	10.845
90	15.392	61.17	111.32	0.188	211.35	17.994	13.83	14.444
120	11.9	67.9	108.3	0.08	209.4	<5,0	7.05	10.5
180 I	17.4	524.4	146.1	0.18	144.8	38.98	7.13	14.7
180 II	12.8	64.1	118.2	0.1	266.8	0.0	6.0	9.9
180 (Blind)	0.486	12.42	0.604	0.147	4.626	19.92	0.796	0.867

Days	Ti	V	Cr	Mn	Fe	Co	Ni	Cu	Zn	As
	[µg/L]	[µg/L]	[µg/L]	[µg/L]	[µg/L]	[µg/L]	[µg/L]	[µg/L]	[µg/L]	[µg/L]
10	1.03	11.79	0.91	0.63	22.44	0.07	1.91	23.15	318.2	9.78
20	1.19	22.28	0.73	0.39	29.32	0.05	1.46	14.33	247.8	8.86
30	0.54	4.99	0.53	0.32	11.79	0.05	1.26	7.85	256	8.84
45	1.138	151.92	0.486	0.909	19.914	0.054	1.516	24	294.4	7.112
60	1.614	18.434	0.651	2.548	33.57	0.105	2.824	14.008	351.4	8.472
90	0.838	178.23	0.366	1.81	13.114	0.063	1.548	16.628	235.4	7.03
120	0.54	24.7	1.384	0.636	14.690	0.104	2.304	15.7	102.42	7.448
180 I	0.79	111.9	0.258	1.336	16.840	0.070	1.638	25.5	107.52	5.254
180 II	0.7	55.6	0.314	0.976	15.636	0.058	1.946	23.7	318.60	7.323
180 (Blind)	0.529	0.209	7.19	454.4	19438	50.76	1236.6	2.134	166.78	1.309

Days	Rb	Sr	Mo	Cd	Sb	Cs	Ba	Pb	U
	[µg/L]	[µg/L]	[µg/L]	[µg/L]	[µg/L]	[µg/L]	[µg/L]	[µg/L]	[µg/L]
10	34.1	75.2	39.5	0.066	1.49	1.64	0.59	0.1	0.024
20	23.9	77.6	54.2	0.082	1.26	0.98	0.35	0.22	0.096
30	24.1	65.3	49.1	0.068	1.42	1.4	0.39	0.06	0.015
45	17.334	142.47	51.54	0.068	1.392	0.518	0.76	0.177	0.114
60	22.48	99.12	47.74	0.074	2.109	1.238	3.741	0.075	0.177
90	20.44	142.77	82.46	0.112	1.749	0.99	0.456	0.108	0.178
120	16.554	100.08	85.00	0.064	2.160	1.160	0.574	0.014	0.174
180 I	15.696	168.40	104.26	0.072	2.432	0.942	0.766	0.024	0.072
180 II	14.314	84.36	126.99	0.130	1.666	1.008	0.554	0.036	0.214
180 (Blind)	2.242	7.84	10.45	0.021	0.086	0.223	20.22	0.222	0.062

Days	Fluorid	Chlorid	Bromid	Nitrat	Phosphat	Sulfat	SiO2	pH
	mg/L	mg/L	mg/L	mg/L	mg/L	mg/L	mg/L	
10	0.231	66.9	n.a.	n.a.	n.a.	8.7	78.75	8.5
20	0.444	42.9	n.a.	n.a.	n.a.	10.3	82.93	8.52
30	0.334	40.6	n.a.	n.a.	n.a.	8.8	72.42	8.52
45	0.416	46.764	n.a.	n.a.	n.a.	15.037	112.76	8.45
60	0.463	99.749	n.a.	n.a.	n.a.	9.892	109.22	8.25
90	0.770	42.501	n.a.	n.a.	n.a.	13.196	113.19	8.25
120	1.846	41.149	n.a.	0.941	n.a.	14.575	108.79	8.3
180 I	5.567	43.406	n.a.	0.947	n.a.	15.617	107.93	7.8
180 II	1.711	38.992	n.a.	0.955	n.a.	19.280	105.78	8.43
180 (Blind)	1.308	1.265	n.a.	n.a.	n.a.	0.598	10.94	5